

Challenges in computing thermal and non-thermal emission from relativistic outflows

Petar Mimica

www.uv.es/mimica Petar.Mimica@uv.es

Department of Astronomy and Astrophysics
University of Valencia

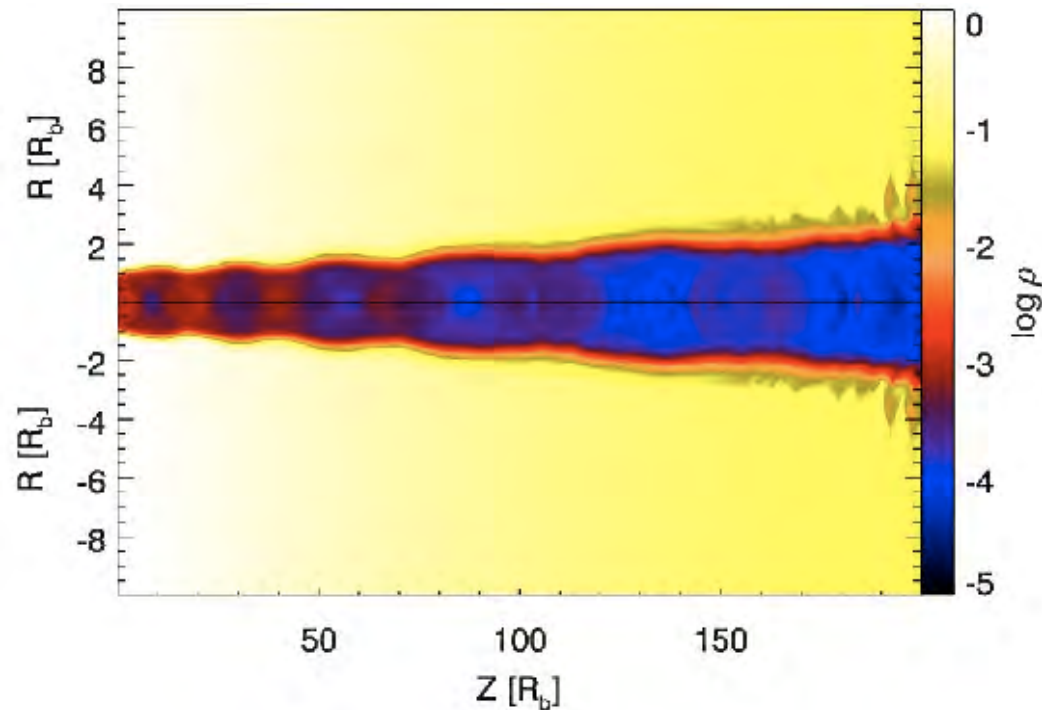
in collaboration with: M.A.Aloy, C. Cuesta-Martínez, C.Aloy



Outline

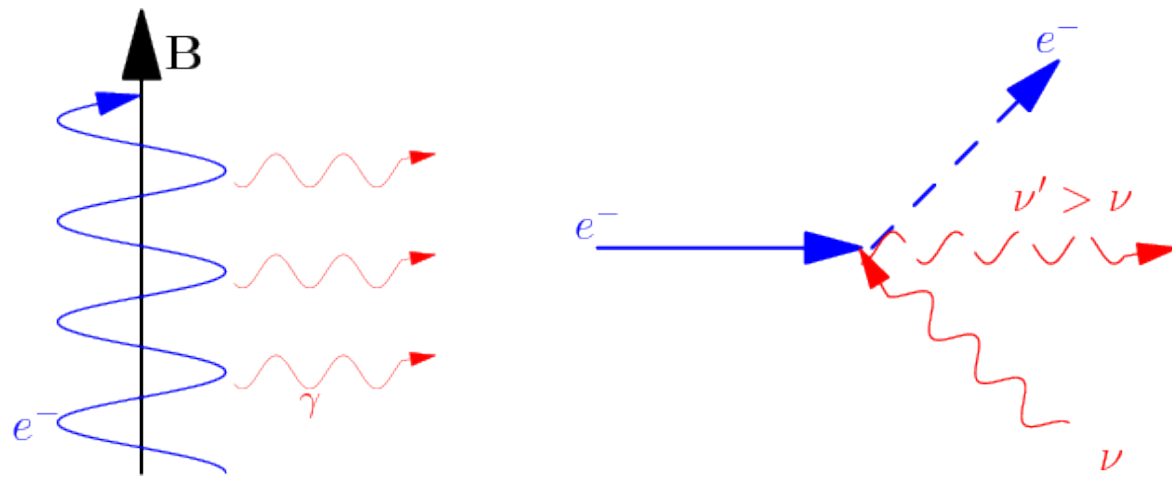
1. Simulating relativistic jets
2. Jets from tidal-disruption events
3. Jets in blackbody dominated GRBs
4. Summary

Simulating relativistic jets



1. relativistic hydrodynamics simulation

- finite-volumes
- method of lines
- shock-capturing
- approximate Riemann solver

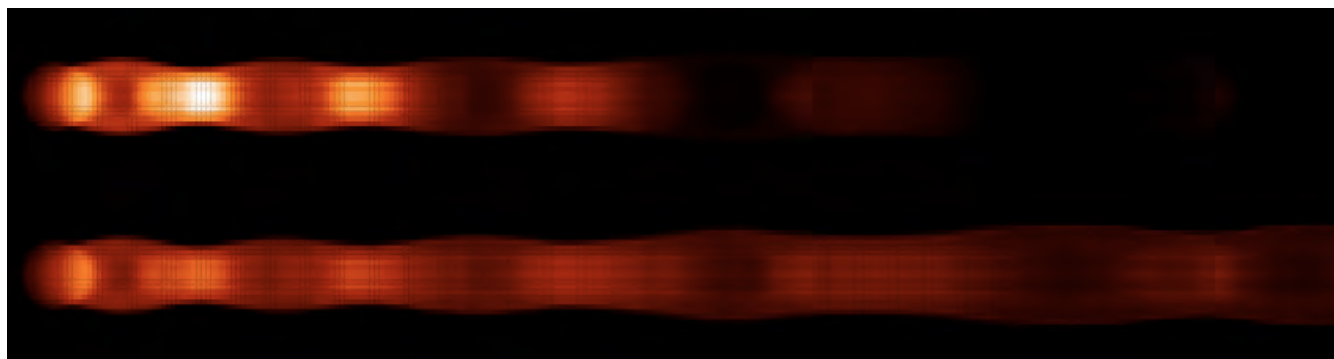


2. non-thermal particle evolution

- phenomenological shock acceleration
- radiative and adiabatic losses
- semi-analytic electron-kinetic eq. solver
- spatial advection

3. radiative transfer

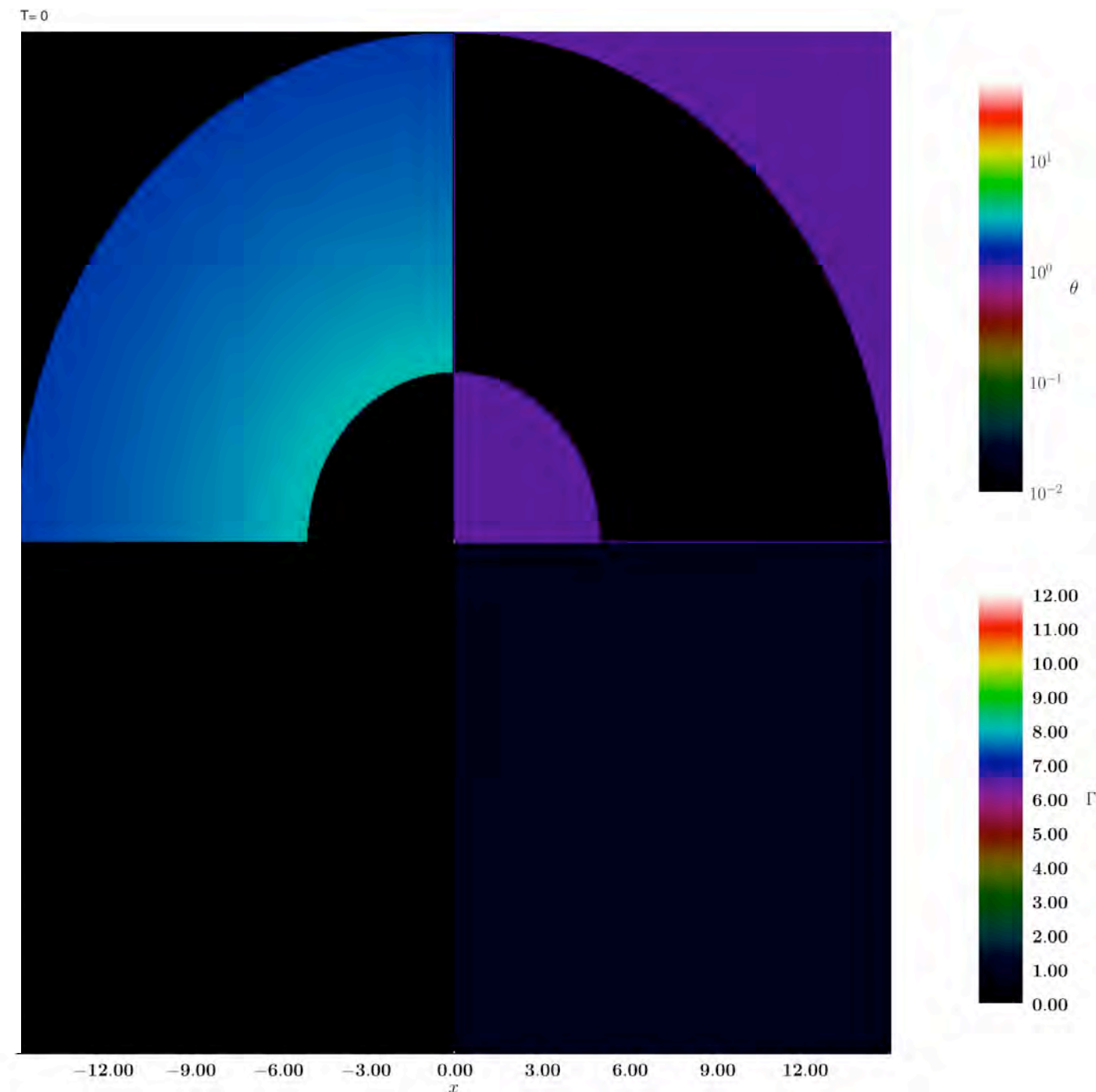
- time-dependent emission and absorption
- relativistic effects (beaming, Doppler)
- light-travel times
- synchrotron, inverse-Compton scattering



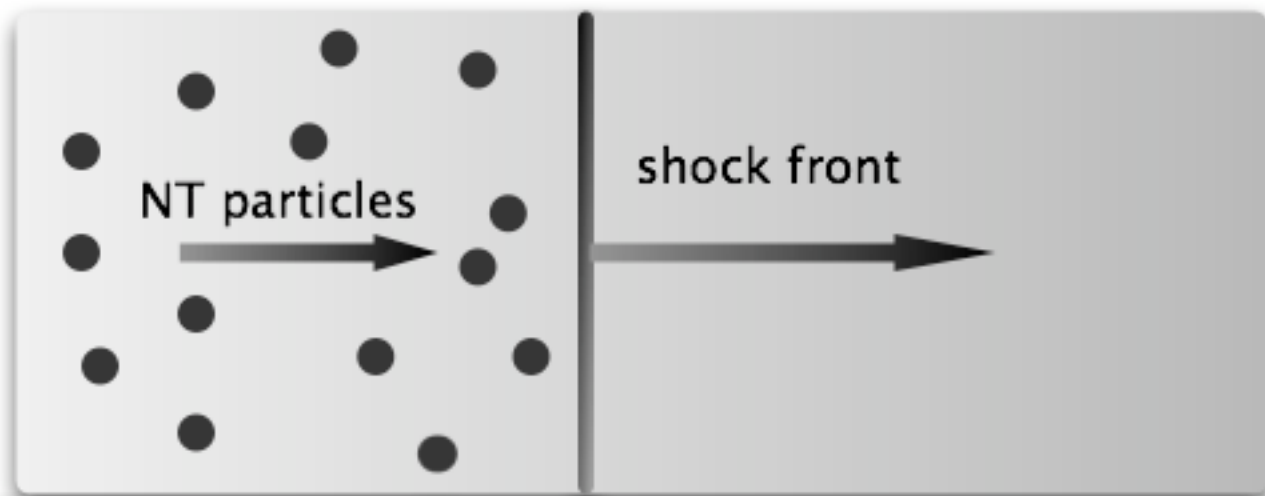
MRGENESIS

MRGENESIS (Aloy *et al.* '99 ApJS , Leismann *et al.* '05, A&A, Mimica *et al.* '07, '09 A&A)

- finite volume approach
- method of lines: separate semi-discretization of space and time
- time advance: TVD Runge-Kutta methods of 2nd and 3rd order
- high-resolution shock-capturing scheme
- inter-cell reconstruction: PPM
- numerical fluxes: Marquina, HLLE, HLLC
- RMHD: constraint transport to conserve $\nabla \mathbf{B}$
- orthogonal coordinate systems: Cartesian, cylindrical, spherical
- MPI + OpenMP: scales up to 10K cores
- HDF5 library for parallel I/O



Non-thermal particles



- model: relativistic shocks accelerate electrons to high energies
- phenomenological source term:

$$Q(\gamma) = Q_0 \gamma^{-s}; \quad \gamma_{\min} \leq \gamma \leq \gamma_{\max}$$

$$\gamma := (1 - v^2/c^2)^{-1/2}$$

electron-kinetic equation $\frac{\partial n(\gamma, t)}{\partial t} + \frac{\partial}{\partial \gamma} (\dot{\gamma} n(\gamma, t)) = Q(\gamma)$

particle energy losses/gains: $\dot{\gamma} = k_a \gamma - k_s \gamma^2$

adiabatic
compression or
expansion

$$k_a = \frac{1}{3} \frac{\mathcal{D} \ln \rho}{\mathcal{D} t}$$

synchrotron
losses

$$k_s = -\frac{4\sigma_T B^2}{3m_e^2 c^2}$$

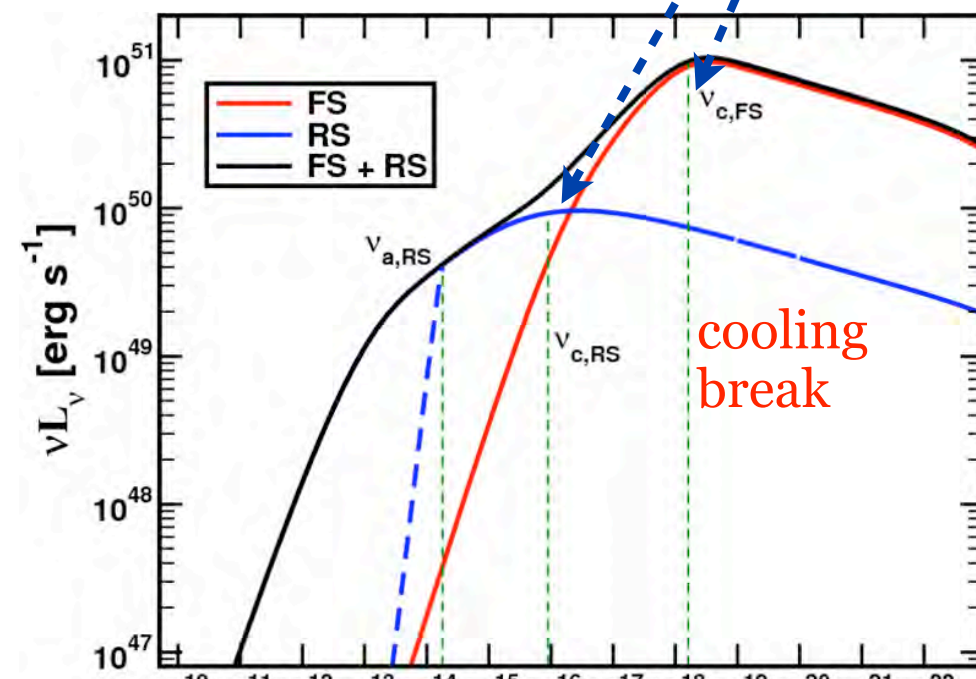
cooling break:
 $\gamma_c(t) = \frac{1}{k_s t}$

fast adaptive bins solver (conserves particle number):

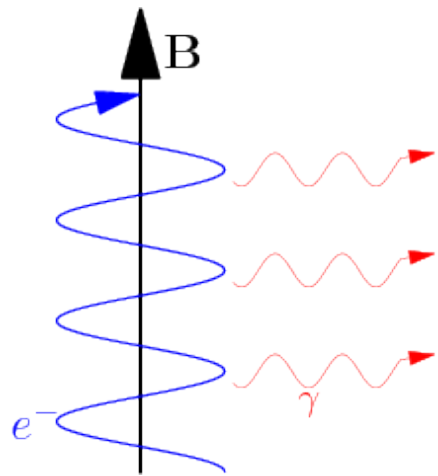
$$\gamma_i(t) = \gamma_i(0) e^{k_a t} \left[1 + \gamma_i(0) \frac{k_s}{k_a} (e^{k_a t} - 1) \right]^{-1}$$

$$n(\gamma_i, t) = n(\gamma_i(0), t) e^{2k_a t} \left[1 + \gamma_i(0) \frac{k_s}{k_a} (e^{k_a t} - 1) \right]^2$$

$$\begin{aligned} \mathcal{N}(\gamma_i, \gamma_{i+1}, t) &:= \int_{\gamma_i}^{\gamma_{i+1}} d\gamma n(\gamma, t) \\ &= e^{3k_a t} \mathcal{N}(\gamma_i(0), \gamma_{i+1}(0), t) \end{aligned}$$



Synchrotron radiation



synchrotron emissivity: $j(\nu) = \frac{\sqrt{3}e^3}{4\pi m_e c^2} \textcolor{red}{B} \int d\gamma \textcolor{blue}{n}(\gamma) R\left(\frac{\nu}{\nu_0 \gamma^2}\right)$

$$\nu_0 = \frac{3e}{4\pi m_e c} \textcolor{red}{B} \quad \textcolor{blue}{n}(\gamma) = n(\gamma_{\min}) \left(\frac{\gamma}{\gamma_{\min}}\right)^{-q} ; \gamma_{\min} \leq \gamma \leq \gamma_{\max}$$

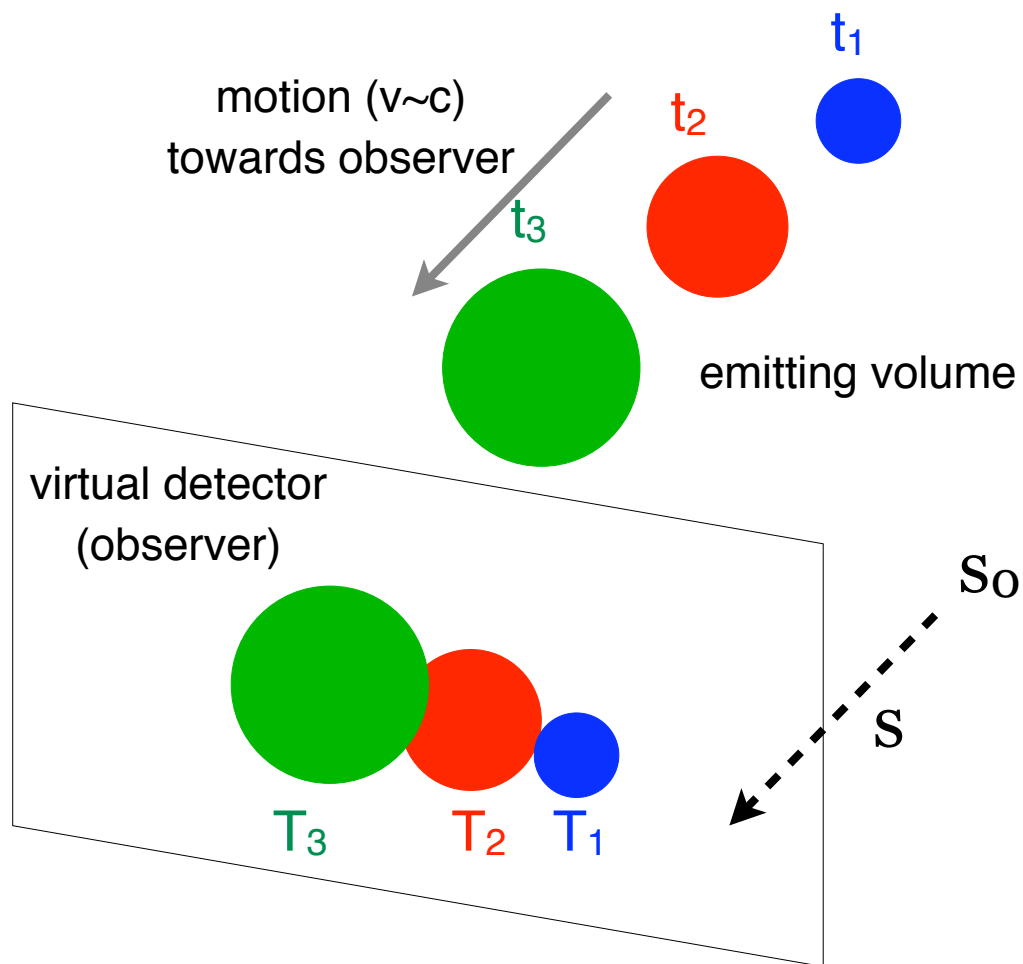
$$R(x) = \frac{1}{2} \int_0^\pi d\alpha \sin^2 \alpha F\left(\frac{x}{\sin \alpha}\right) \quad F(x) = x \int_x^\infty d\xi K_{5/3}(\xi)$$

$$j(\nu) = \frac{\sqrt{3}e^3 B}{8\pi m_e c^2} n(\gamma_{\min}) \gamma_{\min}^q \left(\frac{\nu}{\nu_0}\right)^{(1-q)/2} H\left(\frac{\nu}{\nu_0 \gamma_{\min}^2}, q, \frac{\gamma_{\max}}{\gamma_{\min}}\right)$$

interpolation of the function: $H(x, q, \eta) = \int_{x/\eta^2}^x d\xi \xi^{(q-3)/2} R(\xi)$

- advantage: synchrotron computation cost reduced by a factor 50-100
- tradeoff: large interpolation table (2GB) needs to reside in RAM

Radiative transfer



- for a fixed observer time T , need to process the **whole** spacetime evolution to compute a **single** virtual image
- tightly coupled, highly non-local problem
- **5D problem**:
 - virtual detector image (x, y)
 - observation time T
 - observation frequency ν
 - contributions along the line of sight s

synchrotron,
inverse-Compton

synchrotron
self-absorption

radiative transfer equation:

$$\frac{dI_\nu}{ds} = j_\nu + \alpha_\nu I_\nu$$

$$s = c(t - T) + s_0$$

I_ν : intensity j_ν : emission, absorption

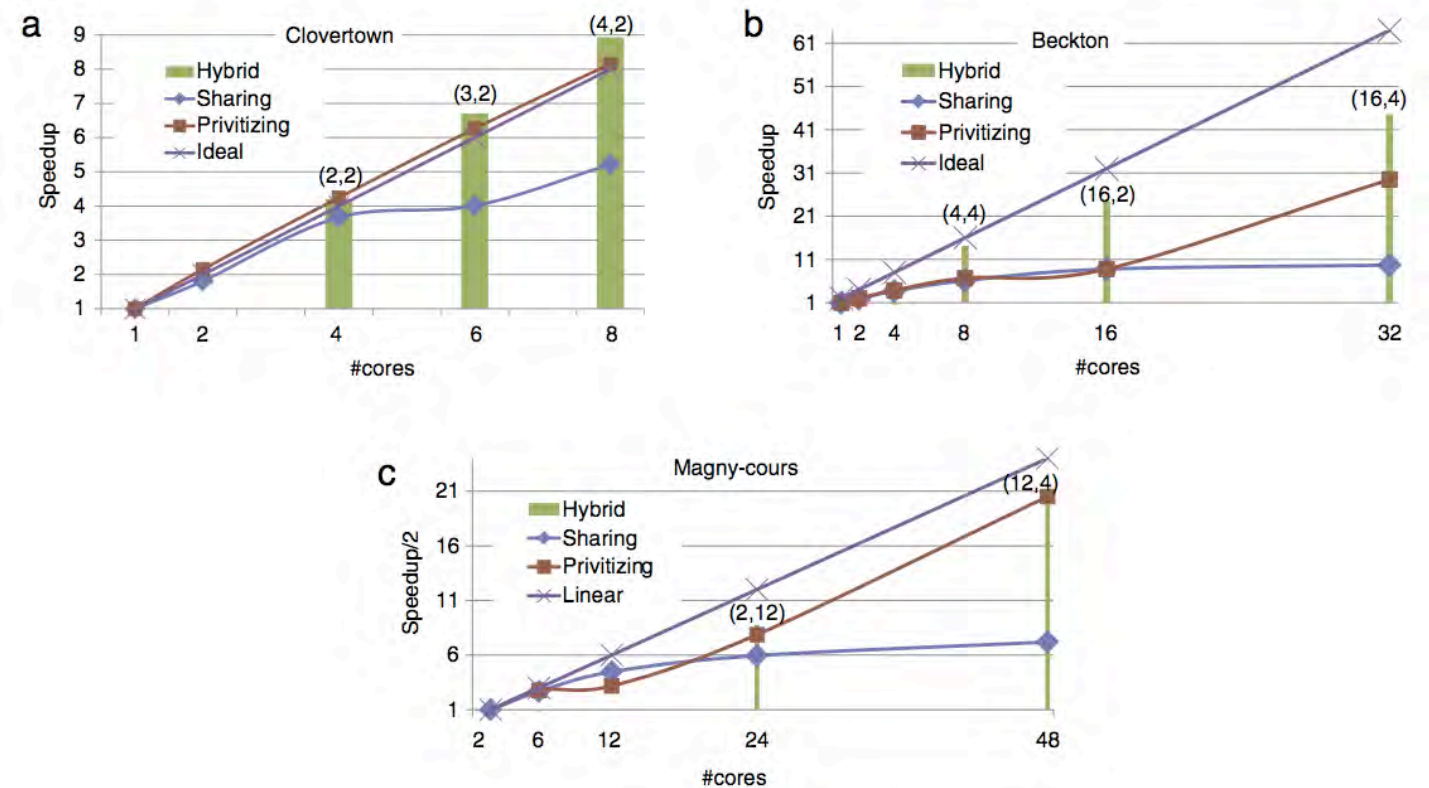
T : observer time t : jet evolution time

s : path towards the detector

for a fixed T , equation gives an isochrone (s, t) along each line of sight

*SP*ectral *EV*olution code

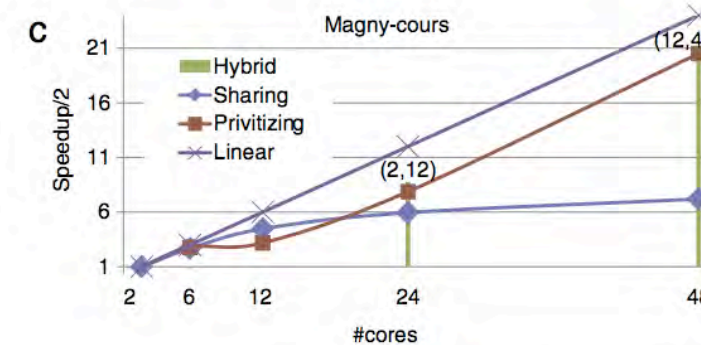
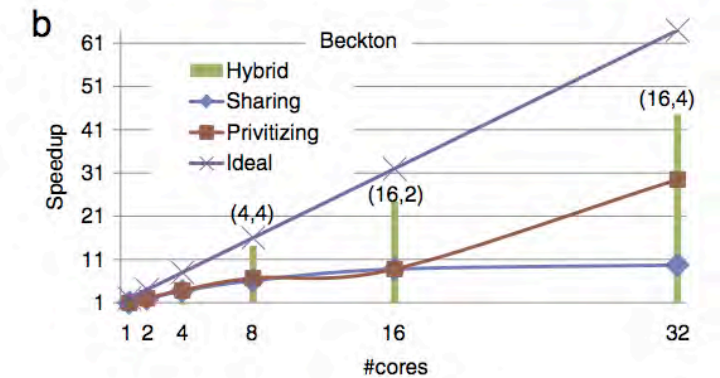
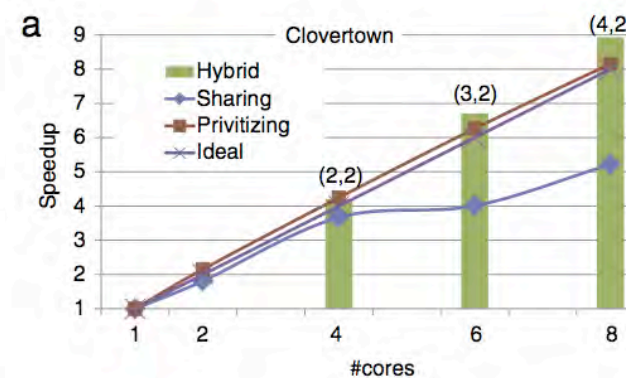
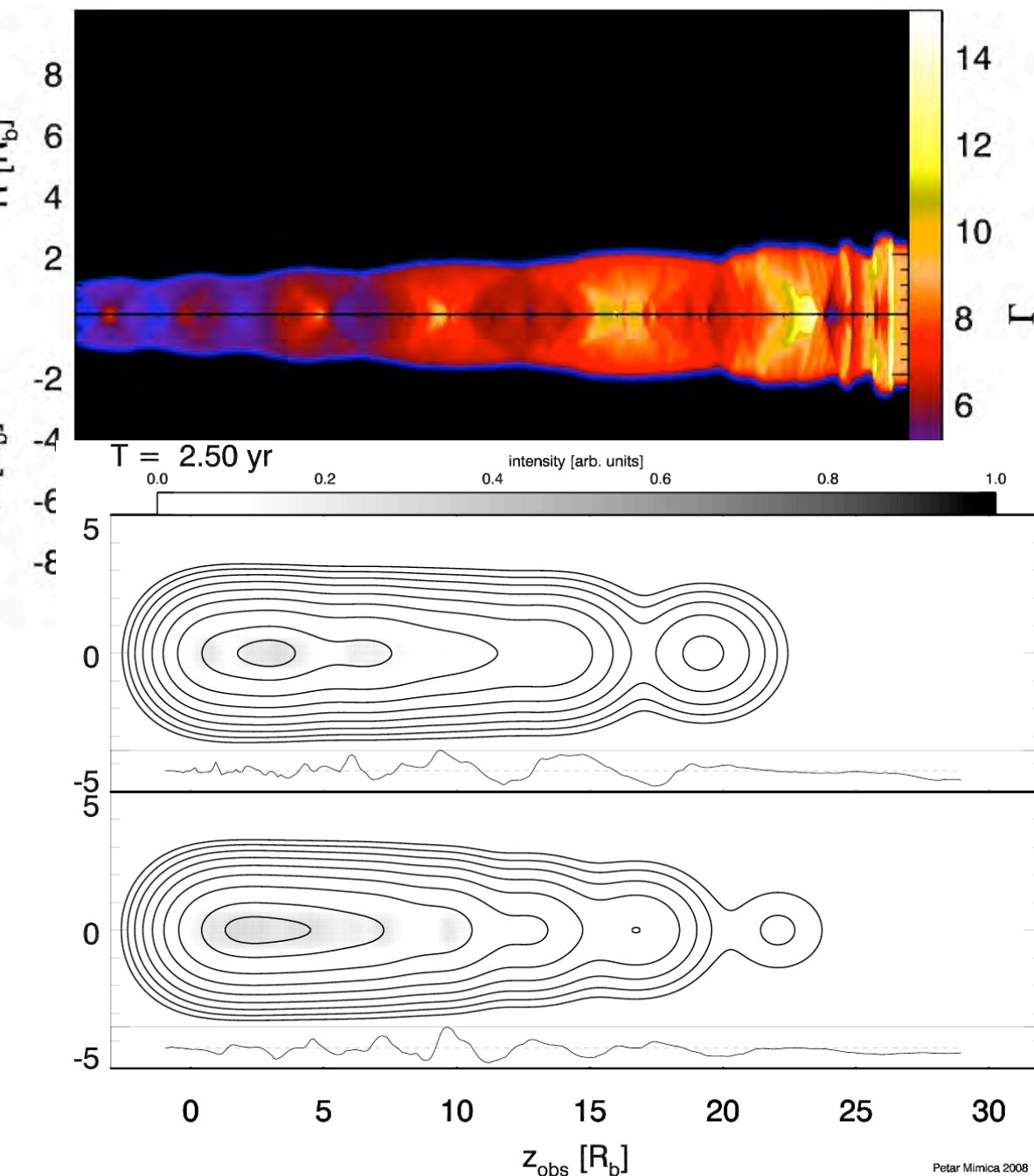
- SPEV (Mimica et al., *Astrophysical J.* **696** (2009) 1142) :
 - non-thermal electron transport and evolution equations
 - time- and frequency-dependent radiative transfer in a dynamically changing background
 - parallelization: MPI (over detector pixels), OpenMP (over particles)



S.Tabik et al. *Computer Physics Communications* **183** (2012) 1937

Spectral EVolution code

- SPEV (Mimica et al., *Astrophysical J.* **696** (2009) 1142) :
 - non-thermal electron transport and evolution equations
 - time- and frequency-dependent radiative transfer in a dynamically changing background
 - parallelization: MPI (over detector pixels), OpenMP (over particles)



S.Tabik et al. *Computer Physics Communications* **183** (2012) 1937

Simulation building blocks

Depending on the application, select one from each row:

RMHD

(GRBs, blazars)

RHD

(AGN jets, TDE jets)

exact Riemann solver

(blazar, GRB internal shocks)

+

3D transport & evolution

(radio maps, off-axis light curves)

Cylindrical

(blazar internal shocks)

Spherical

(on-axis GRB blast wave)

+

Synchrotron (+ EC)

(radio maps, blazar X light curves, GRB afterglows, TDE radio transients)

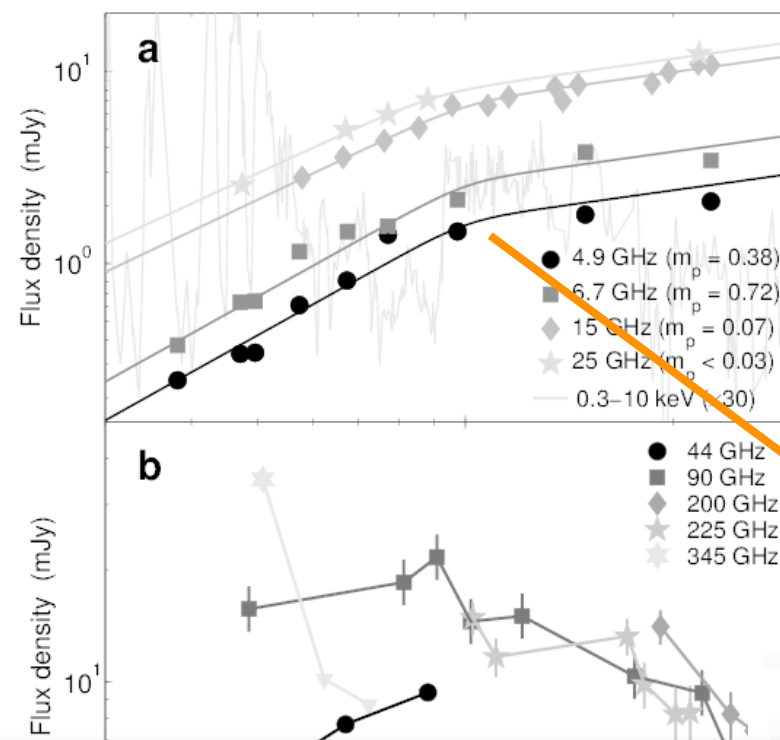
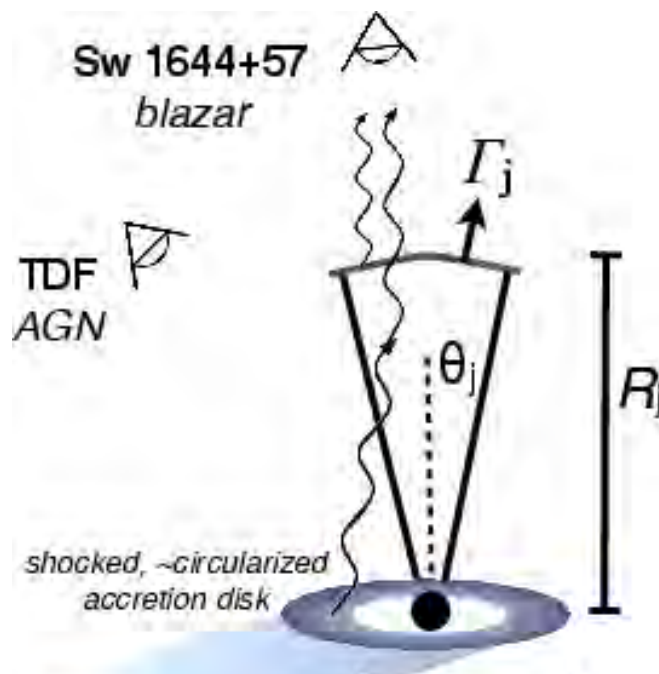
Synchrotron self-Compton

(blazar radio-to- γ -ray light curves and spectra)

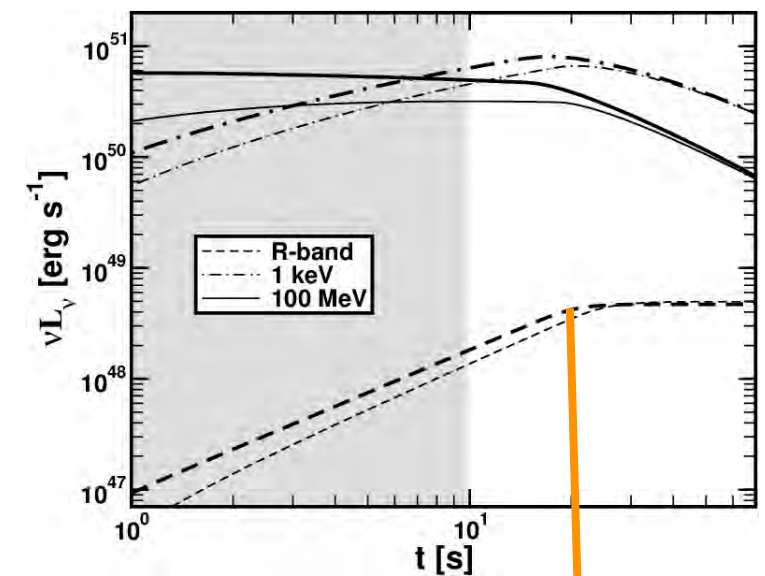
Swift J1644+57

- Swift J164449.31573451 ($z = 0.354$), initially identified as GRB110328A
- longevity of its afterglow points to a different explanation: a blazar-like jet fed by a tidal disruption of a solar-mass star

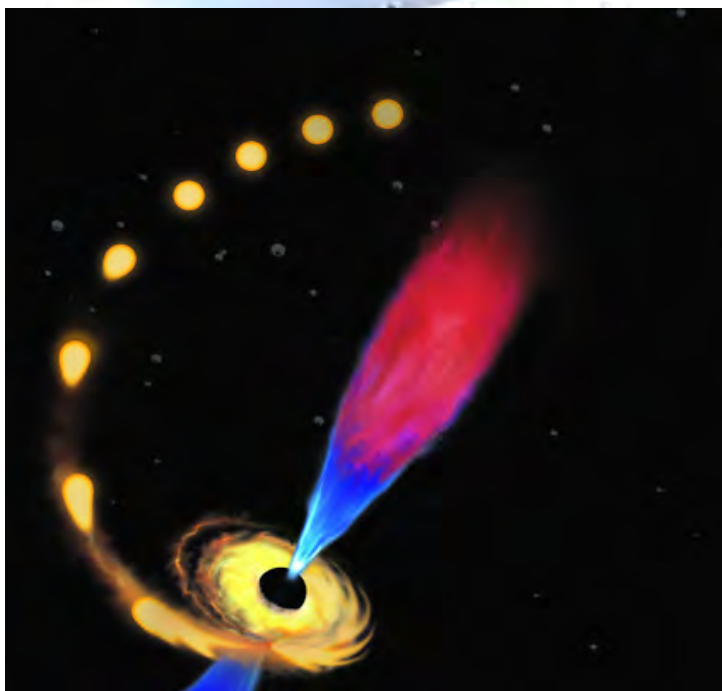
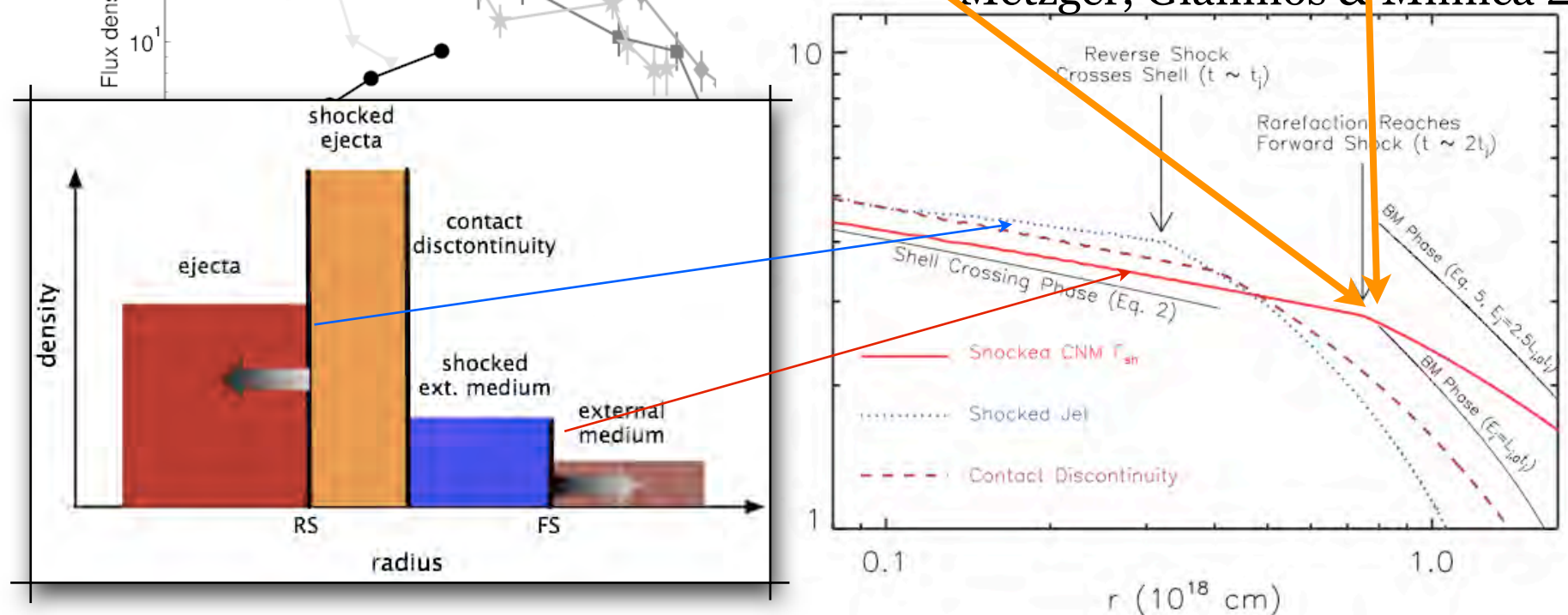
Zauderer *et al.* 2011



Mimica, Giannios & Aloy 2010



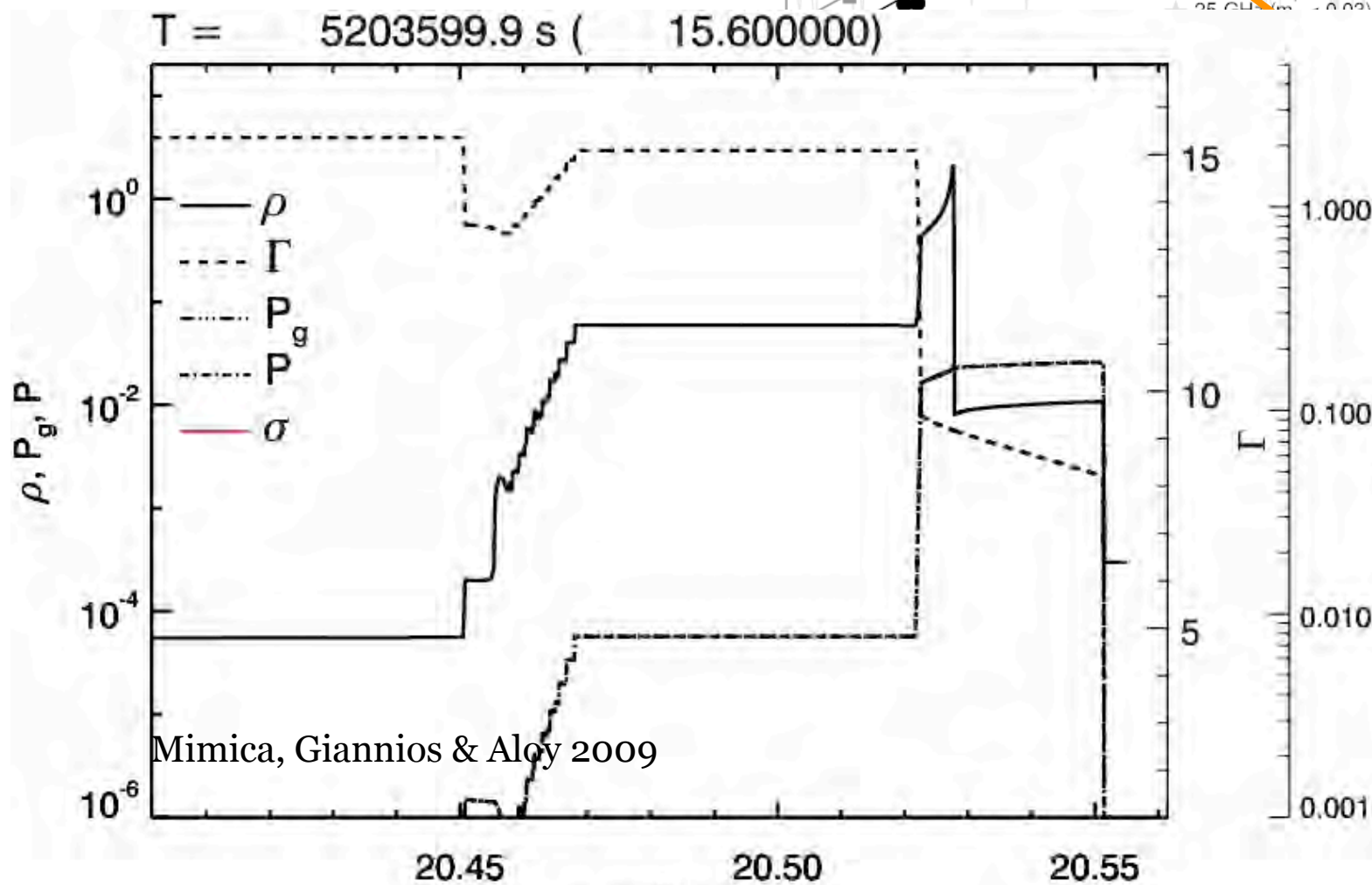
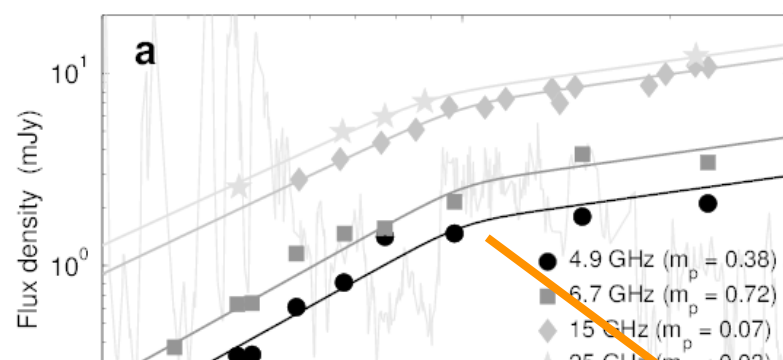
Metzger, Giannios & Mimica 2012



Swift J1644+57

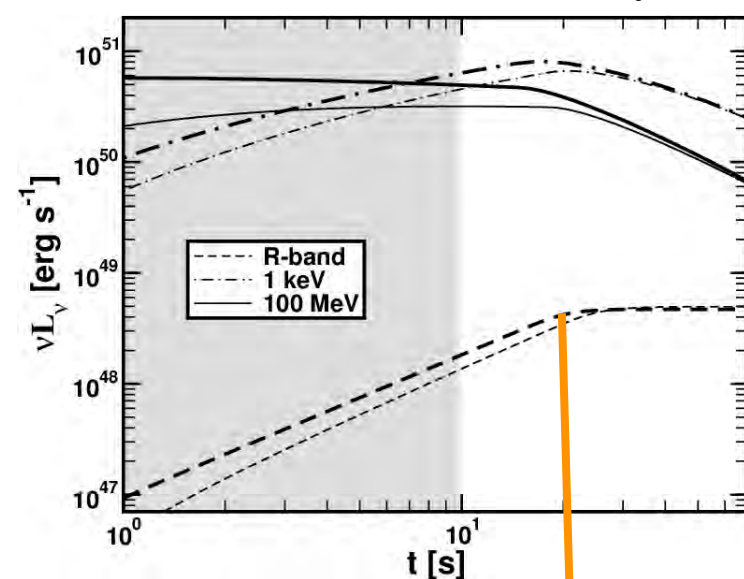
- Swift J164449.31573451 ($z = 0.354$), initially identified as GRB110328A
- longevity of its afterglow points to a different explanation: a blazar-like jet fed by a tidal disruption of a solar-mass star

Zauderer *et al.* 2011

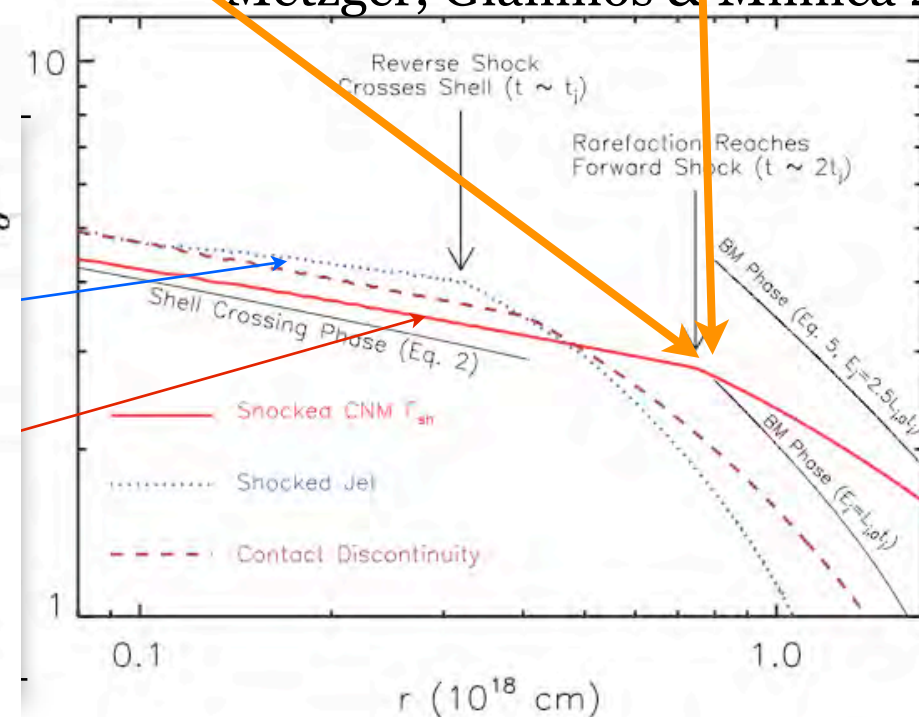


Mimica, Giannios & Aloy 2009

Mimica, Giannios & Aloy 2010



Metzger, Giannios & Mimica 2012



RHD simulations of TDE jets

Physical model

$$L_j(t) = L_{j,0} \left(\max \left[1, \left(\frac{t}{t_{j,0}} \right) \right] \right)^{-5/3}$$

$$L_{j,0} = 5 \times 10^{47} \text{ erg s}^{-1}$$

$$t_{j,0} = 5 \times 10^5 \text{ s}$$

$$\Gamma_{j,0} = 5 \quad \theta_{j,0} = 0.3 \text{ rad}$$

$$\Theta_0 := \frac{P_0}{\rho_0 c^2} = 10^{-2}$$

$$\text{TM EOS : } h(\Theta) = \frac{5}{2}\Theta + \sqrt{\frac{9}{4}\Theta^2 + 1}$$

(Mignone *et al.* 05)

$$R_{j,0} = 5 \times 10^{16} \text{ cm}$$

$$n_{\text{ext}}(R) = 3.33 \times 10^1 \text{ cm}^{-3} \left(\frac{R}{R_{j,0}} \right)^{-1}$$

$$T_{\text{max}} \approx 15 \text{ years}$$

thermal density

Lorentz factor

non-thermal density

synchrotron peak

RHD simulations of TDE jets

Physical model

$$L_j(t) = L_{j,0} \left(\max \left[1, \left(\frac{t}{t_{j,0}} \right) \right] \right)^{-5/3}$$

$$L_{j,0} = 5 \times 10^{47} \text{ erg s}^{-1}$$

$$t_{j,0} = 5 \times 10^5 \text{ s}$$

$$\Gamma_{j,0} = 5 \quad \theta_{j,0} = 0.3 \text{ rad}$$

$$\Theta_0 := \frac{P_0}{\rho_0 c^2} = 10^{-2}$$

$$\text{TM EOS : } h(\Theta) = \frac{5}{2}\Theta + \sqrt{\frac{9}{4}\Theta^2 + 1}$$

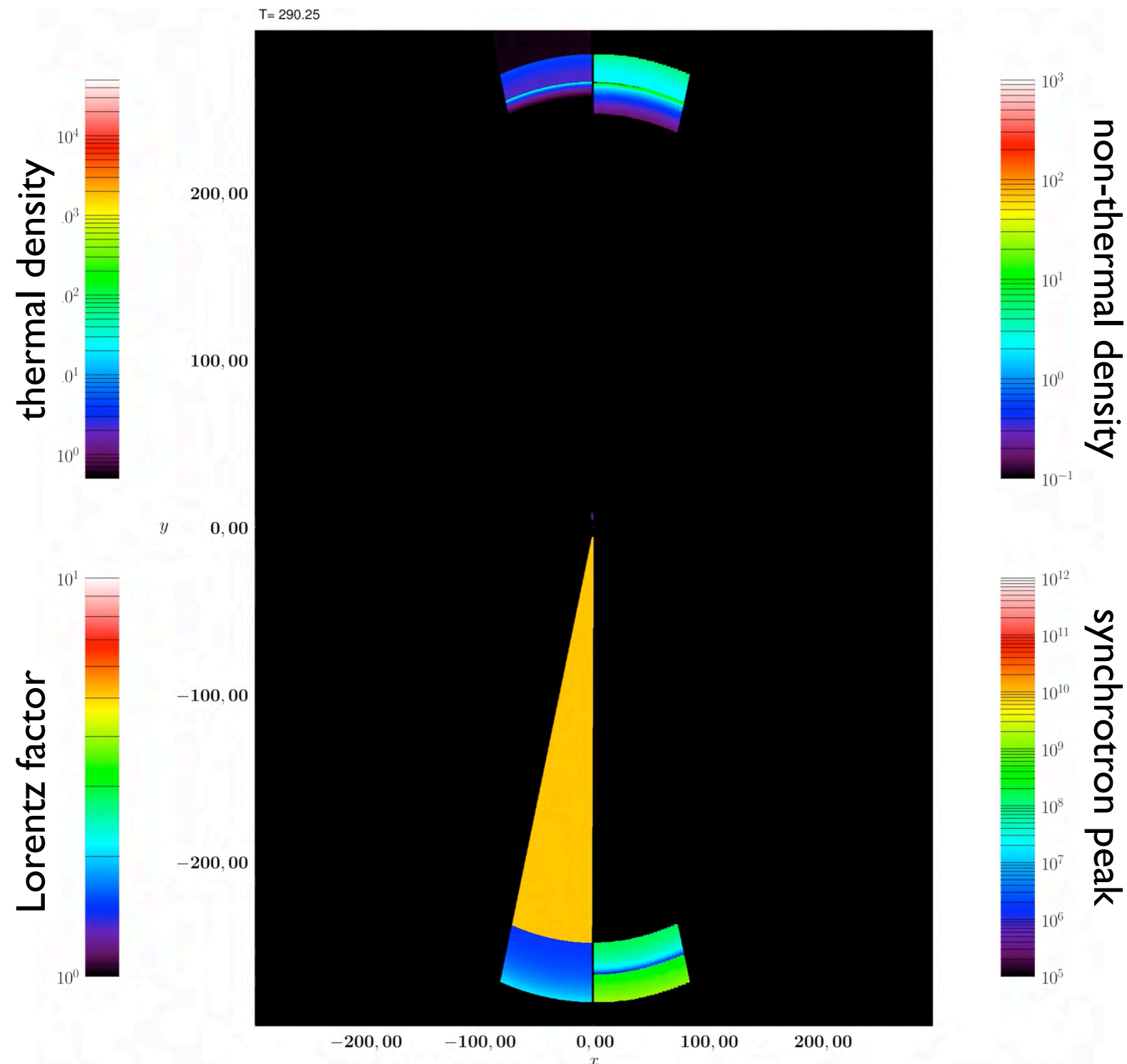
(Mignone et al. 05)

$$R_{j,0} = 5 \times 10^{16} \text{ cm}$$

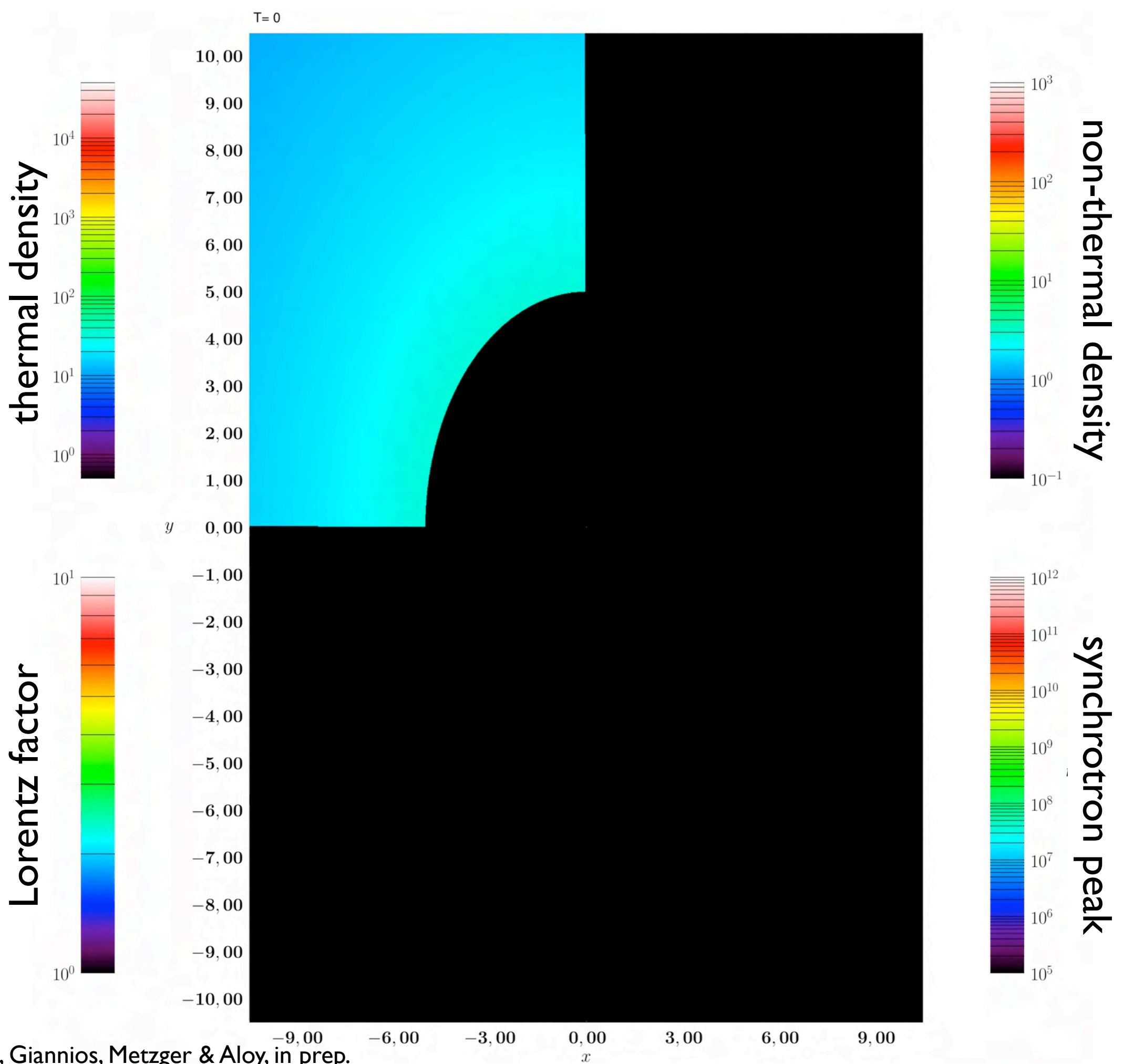
$$n_{\text{ext}}(R) = 3.33 \times 10^1 \text{ cm}^{-3} \left(\frac{R}{R_{j,0}} \right)^{-1}$$

$$T_{\text{max}} \approx 15 \text{ years}$$

Mimica, Giannios, Metzger & Aloy, in prep.



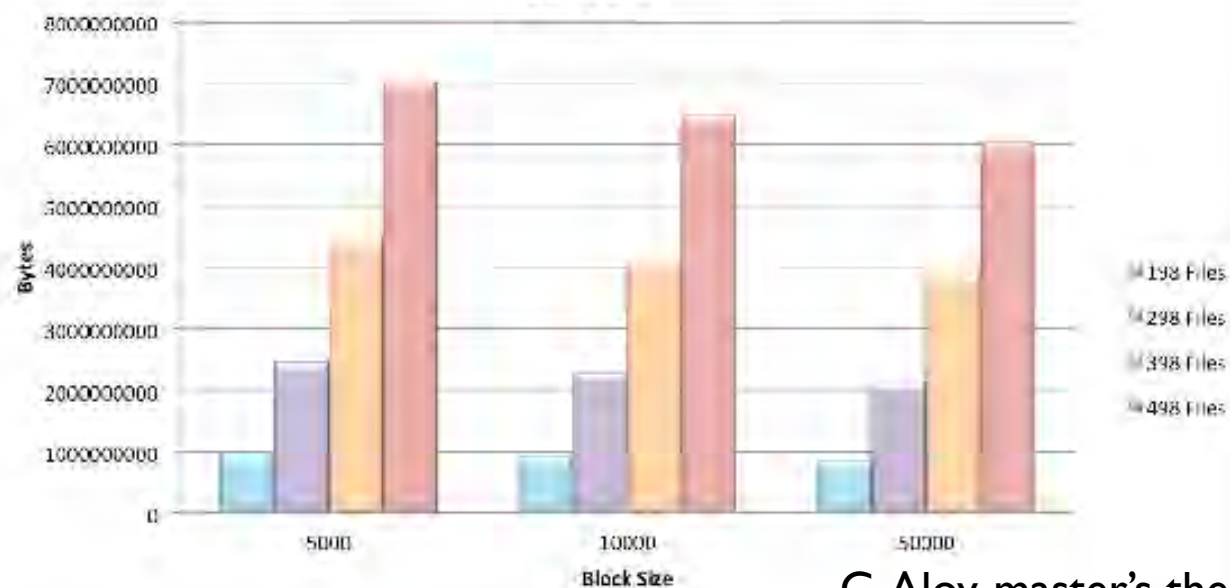
2D RHD simulation



Light curves and technical details

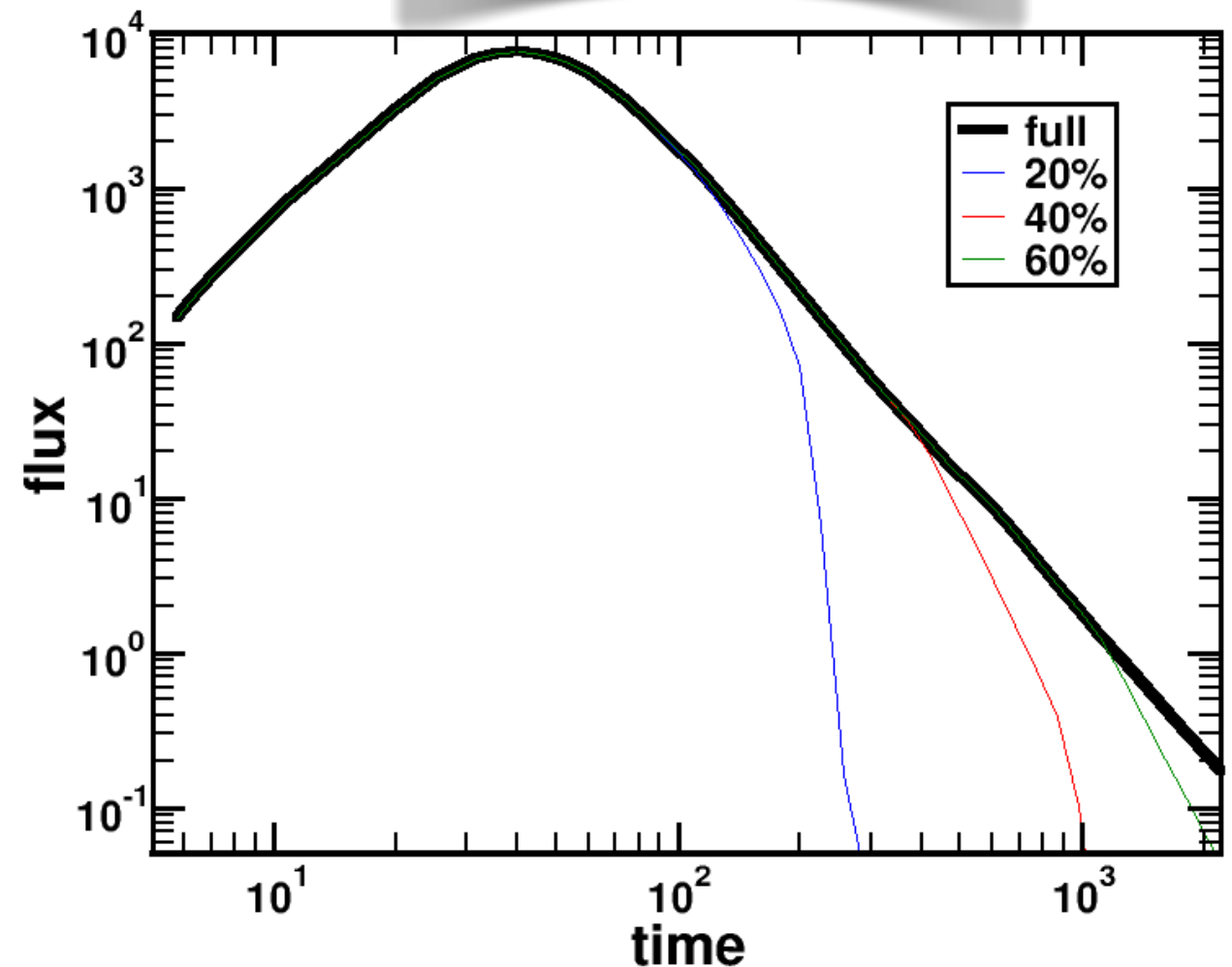
Technical details

- uniform spherical grid, 2D resolution 54000 x 250 (12 million numerical cells)
- 1400 snapshots: dense linear coverage (600 snap.) until 1.6 yr; progressively increasing intervals (800 snap.) 1.6 - 15 yr
- dense coverage in time necessary to correctly compute the light curves
- total res.: $54000 \times 250 \times 1400 = 1.89 \cdot 10^{10}$
- 3D estimate: $2 \cdot 10^{12}$ points
- tens to hundreds of GB of shared RAM (machine *LluísVives* at UV, 114 cores)
- size of the intermediate files increases quadratically with number of snapshots!



C.Aloy, master's thesis

Radio light curve

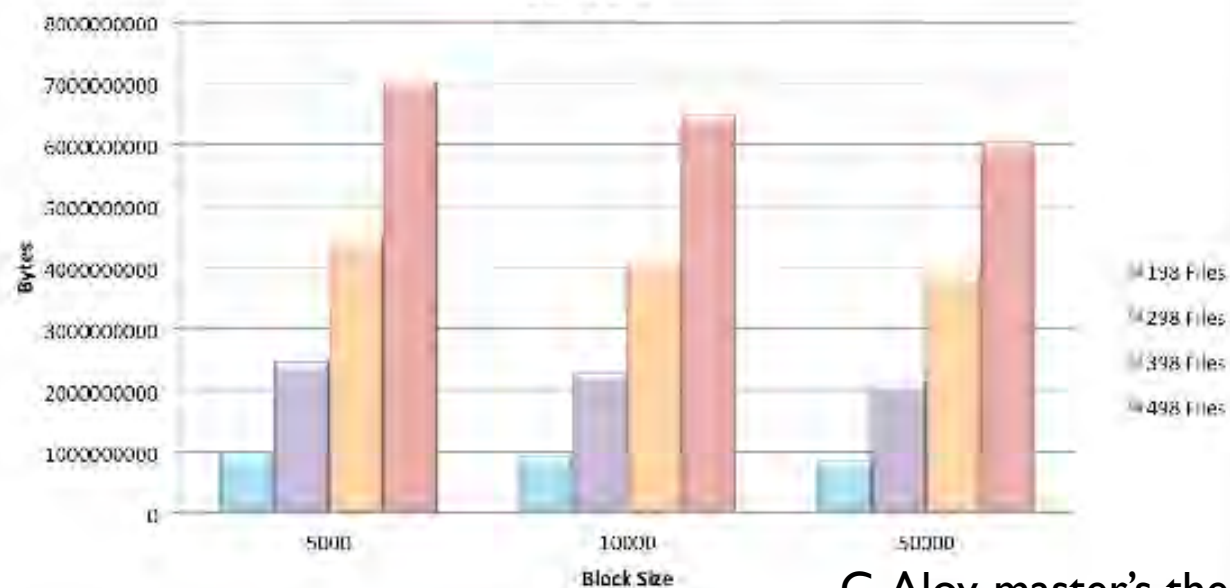


- 10^6 non-thermal emitting regions (32 bins)
- enough space-time coverage is crucial for correct light curve computation
- extension of the duration of the light curve requires disproportionately more computation time and storage space!

Light curves and technical details

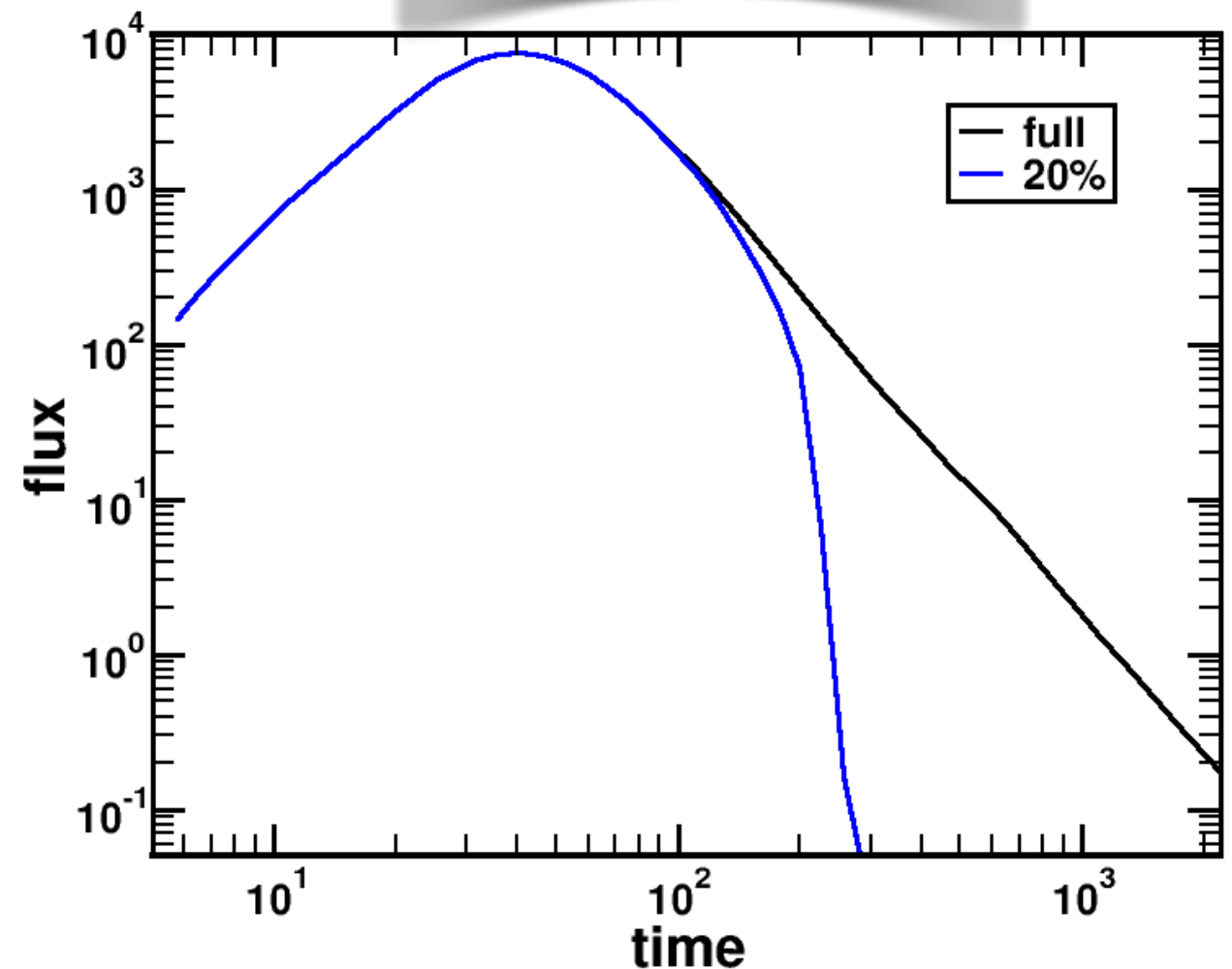
Technical details

- uniform spherical grid, 2D resolution 54000 x 250 (12 million numerical cells)
- 1400 snapshots: dense linear coverage (600 snap.) until 1.6 yr; progressively increasing intervals (800 snap.) 1.6 - 15 yr
- dense coverage in time necessary to correctly compute the light curves
- total res.: $54000 \times 250 \times 1400 = 1.89 \cdot 10^{10}$
- 3D estimate: $2 \cdot 10^{12}$ points
- tens to hundreds of GB of shared RAM (machine *LluisVives* at UV, 114 cores)
- size of the intermediate files increases quadratically with number of snapshots!



C.Aloy, master's thesis

Radio light curve

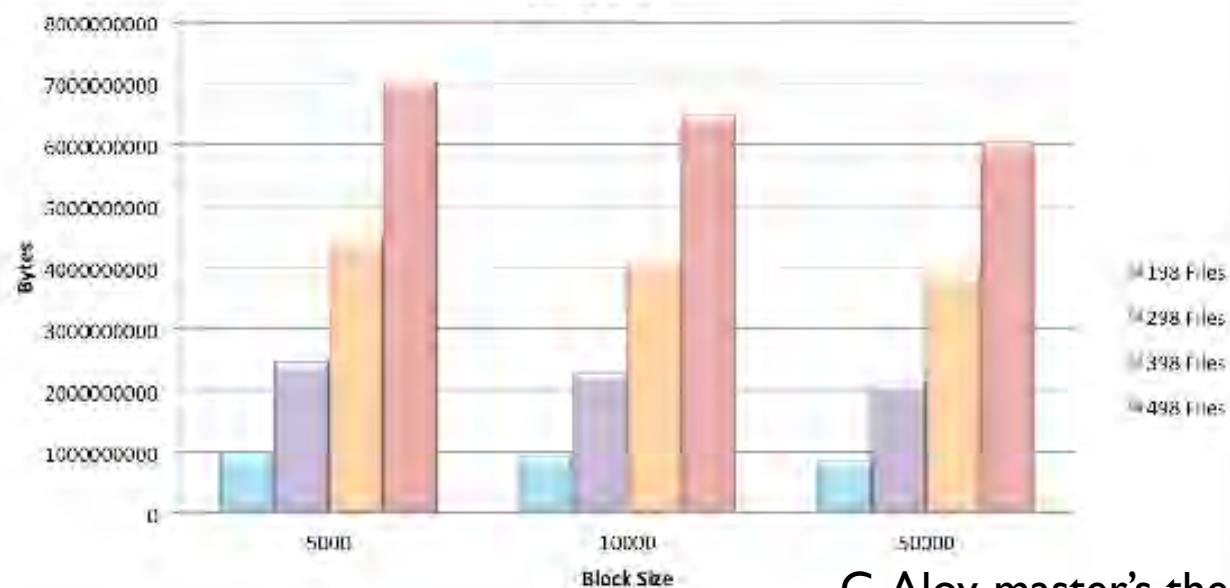


- 10^6 non-thermal emitting regions (32 bins)
- enough space-time coverage is crucial for correct light curve computation
- extension of the duration of the light curve requires disproportionately more computation time and storage space!

Light curves and technical details

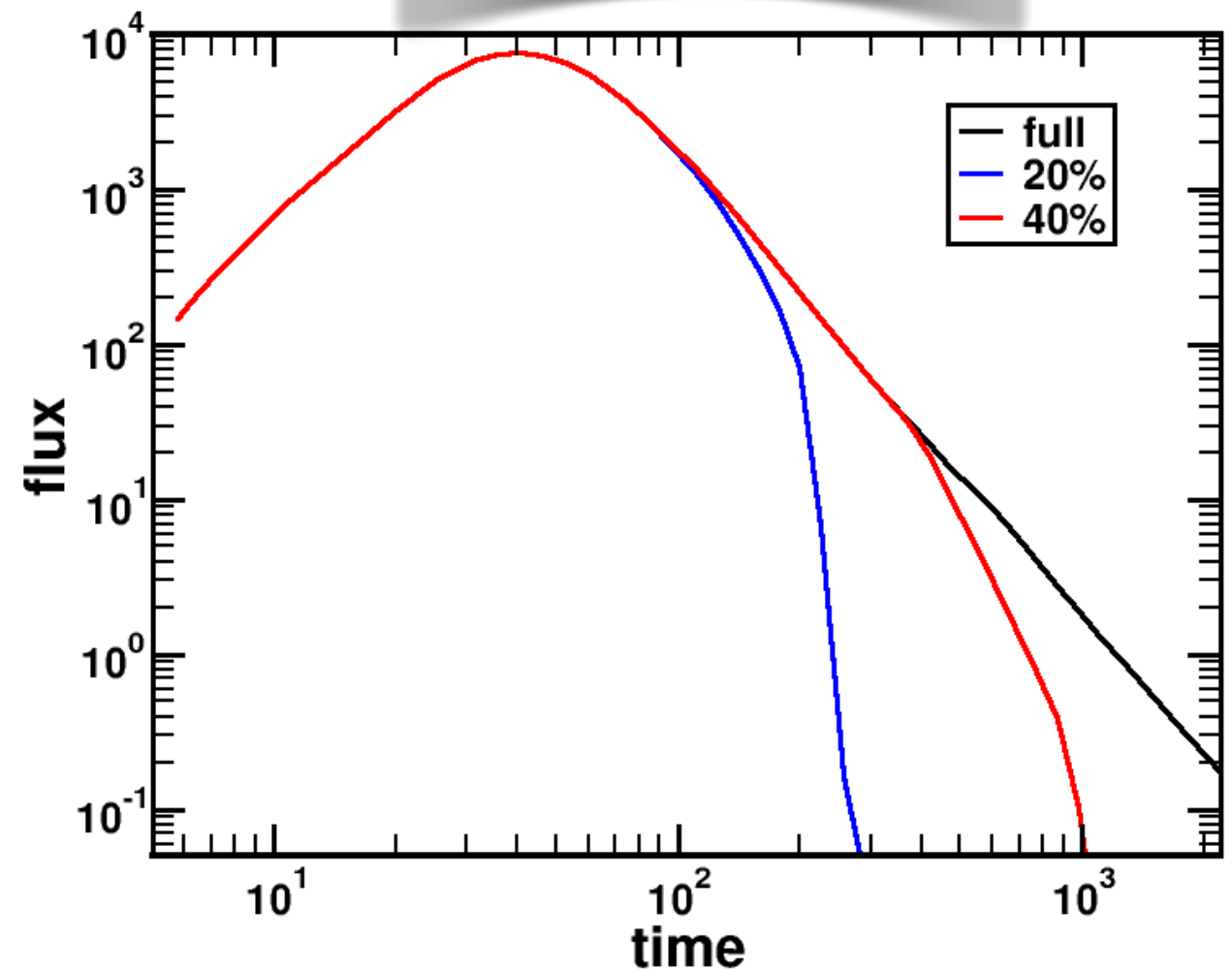
Technical details

- uniform spherical grid, 2D resolution 54000 x 250 (12 million numerical cells)
- 1400 snapshots: dense linear coverage (600 snap.) until 1.6 yr; progressively increasing intervals (800 snap.) 1.6 - 15 yr
- dense coverage in time necessary to correctly compute the light curves
- total res.: $54000 \times 250 \times 1400 = 1.89 \cdot 10^{10}$
- 3D estimate: $2 \cdot 10^{12}$ points
- tens to hundreds of GB of shared RAM (machine *LluísVives* at UV, 114 cores)
- size of the intermediate files increases quadratically with number of snapshots!



C.Aloy, master's thesis

Radio light curve

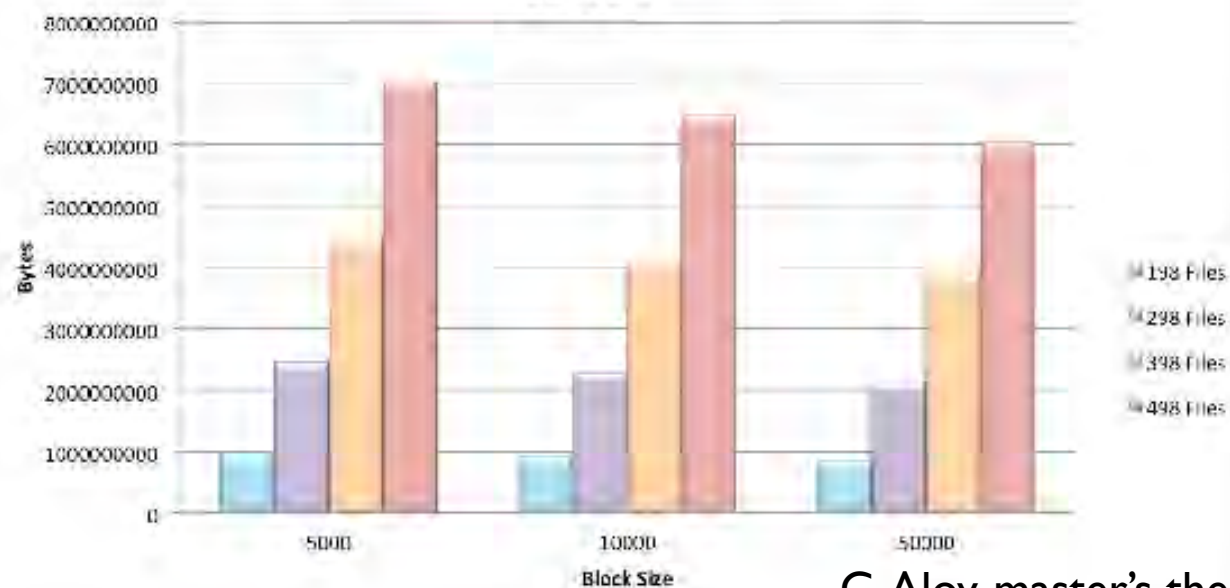


- 10^6 non-thermal emitting regions (32 bins)
- enough space-time coverage is crucial for correct light curve computation
- extension of the duration of the light curve requires disproportionately more computation time and storage space!

Light curves and technical details

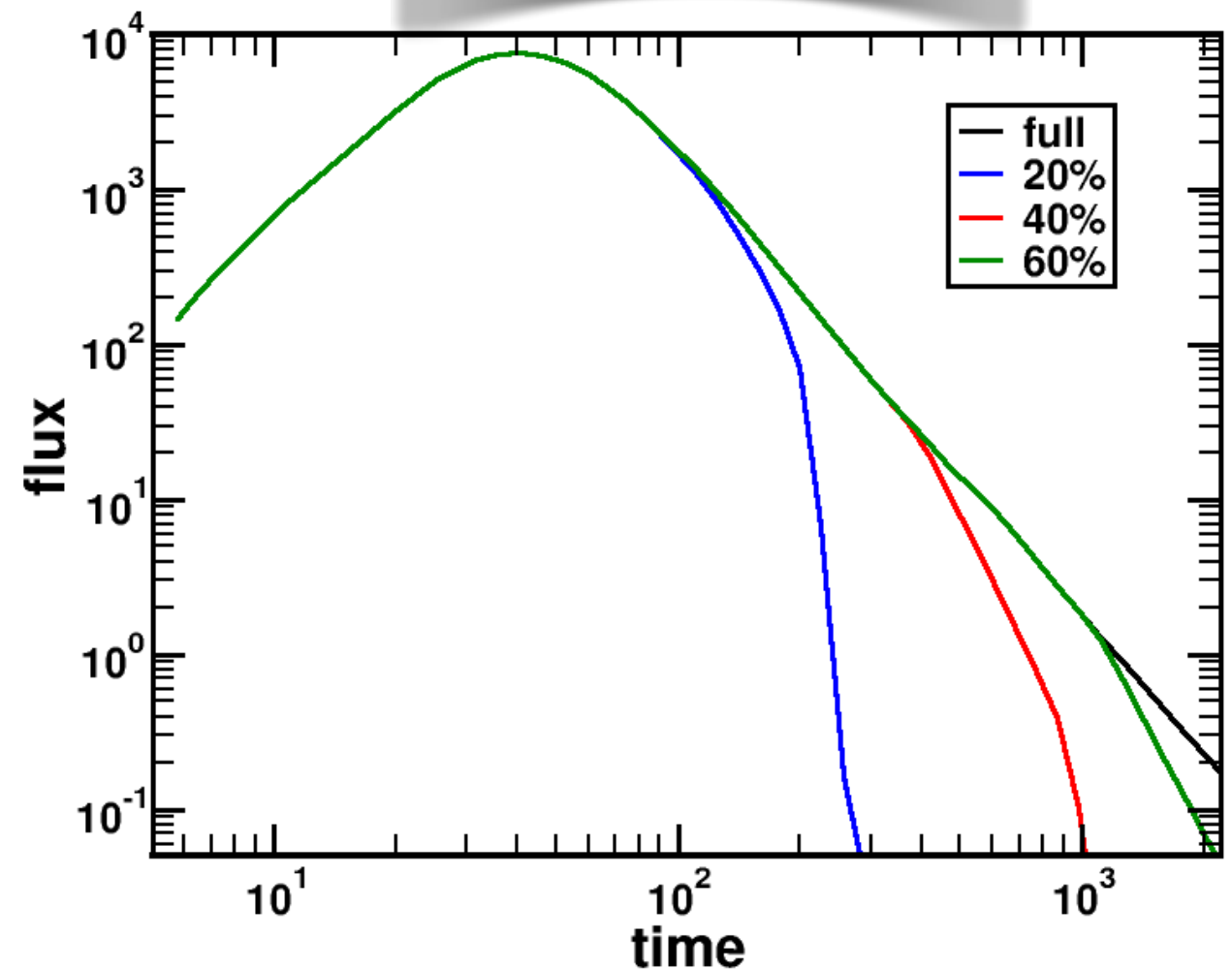
Technical details

- uniform spherical grid, 2D resolution 54000 x 250 (12 million numerical cells)
- 1400 snapshots: dense linear coverage (600 snap.) until 1.6 yr; progressively increasing intervals (800 snap.) 1.6 - 15 yr
- dense coverage in time necessary to correctly compute the light curves
- total res.: $54000 \times 250 \times 1400 = 1.89 \cdot 10^{10}$
- 3D estimate: $2 \cdot 10^{12}$ points
- tens to hundreds of GB of shared RAM (machine *LluisVives* at UV, 114 cores)
- size of the intermediate files increases quadratically with number of snapshots!



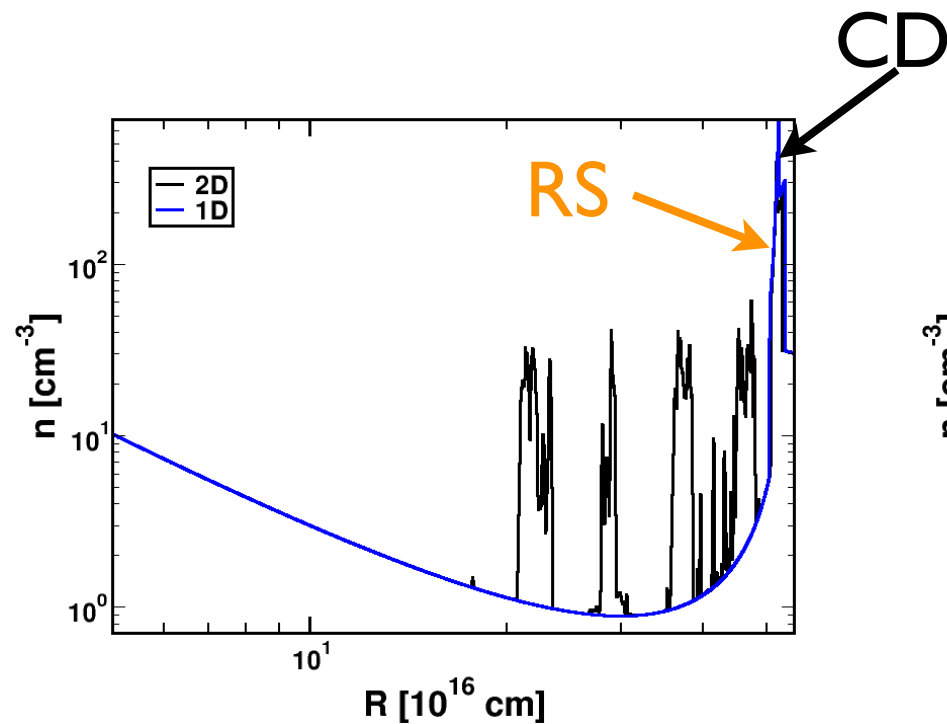
C.Aloy, master's thesis

Radio light curve

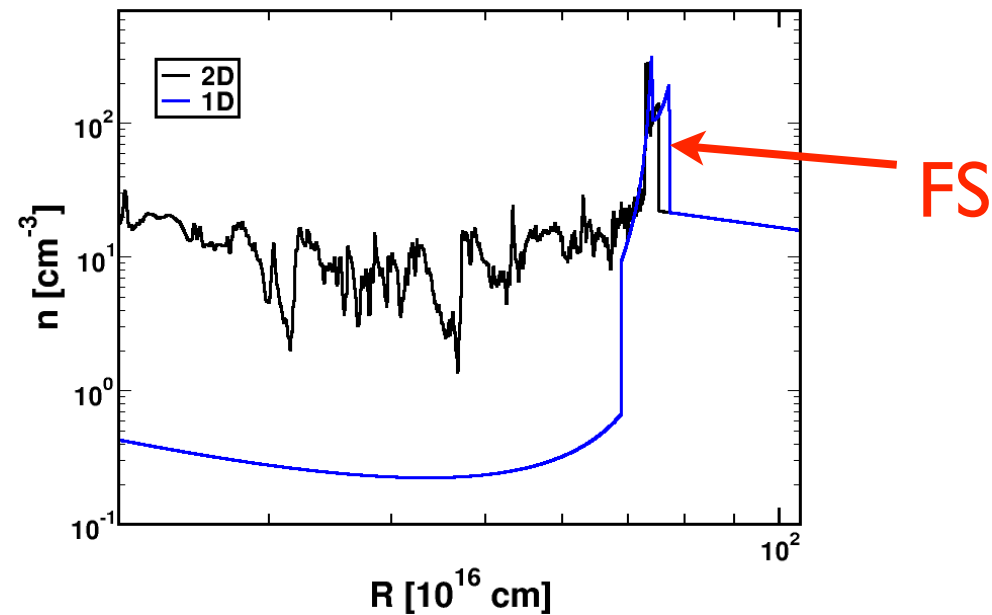


- 10^6 non-thermal emitting regions (32 bins)
- enough space-time coverage is crucial for correct light curve computation
- extension of the duration of the light curve requires disproportionately more computation time and storage space!

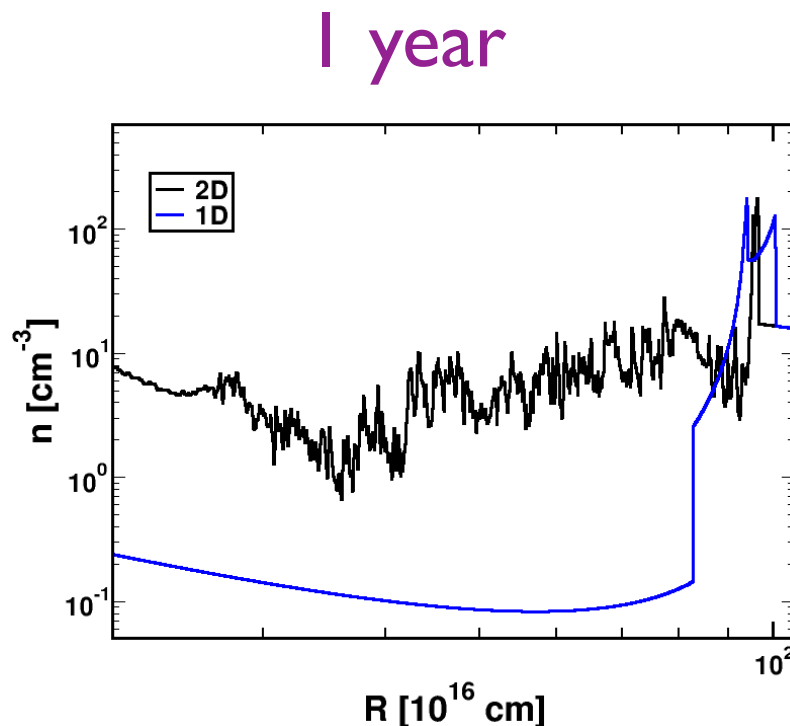
1D versus 2D



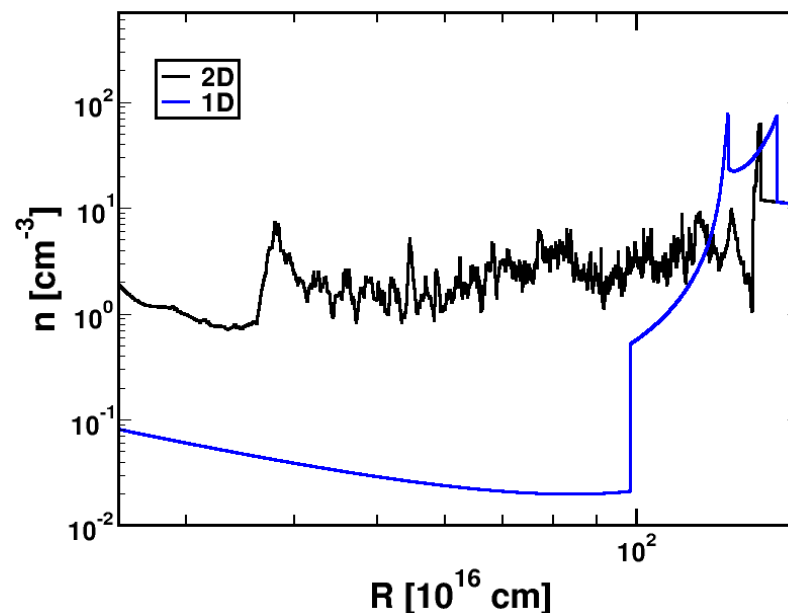
0.5 years



0.8 years



1 year



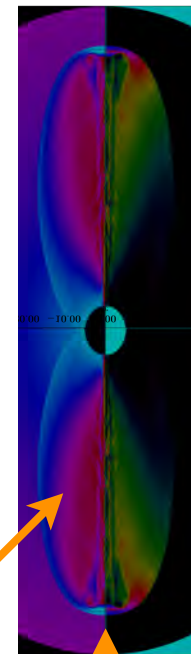
1.6 years

off-axis obs.

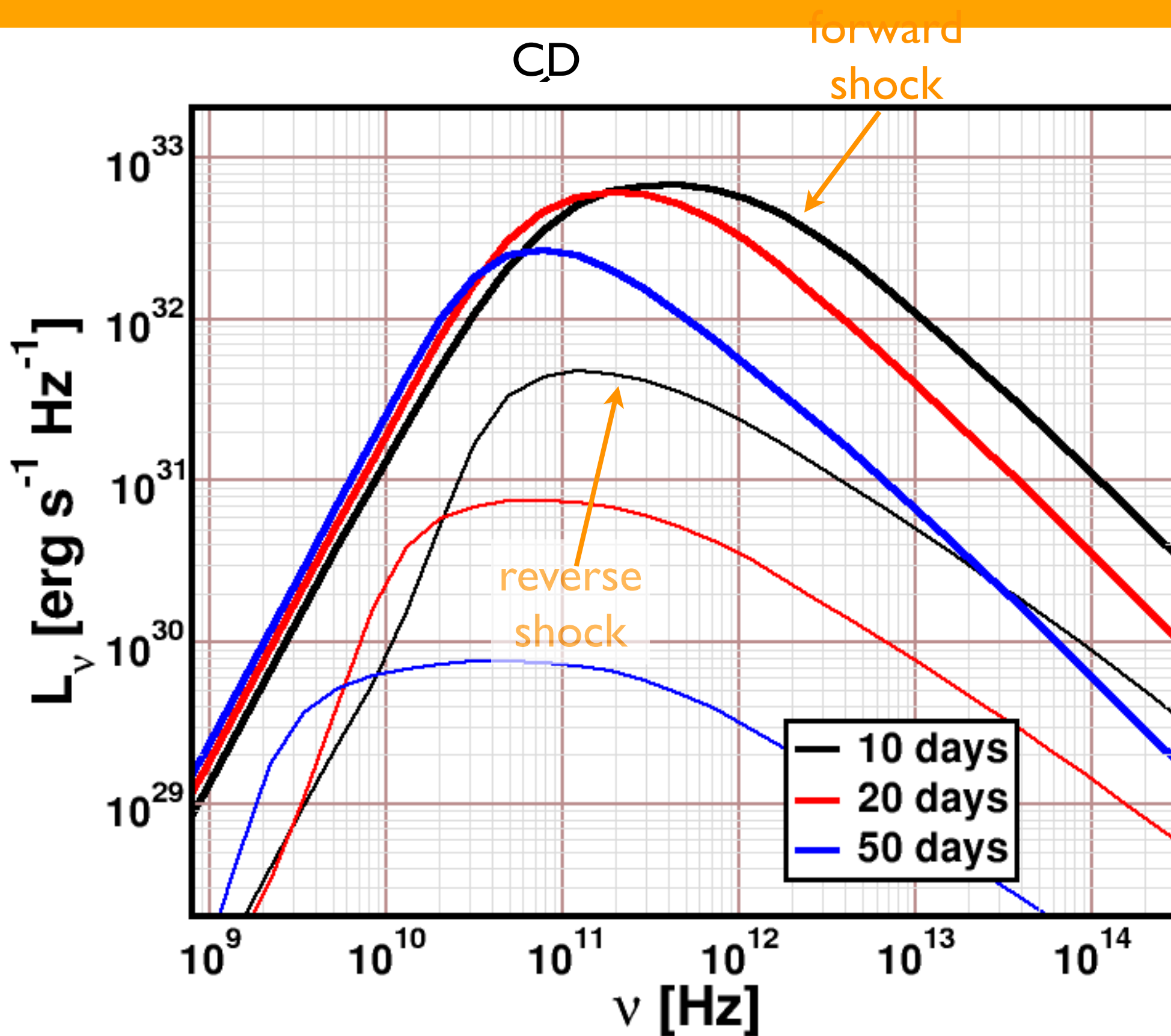
- radio maps, spectra
- light curves

on-axis obs.

- 1D - 2D comparison
- comparison with J1644+57

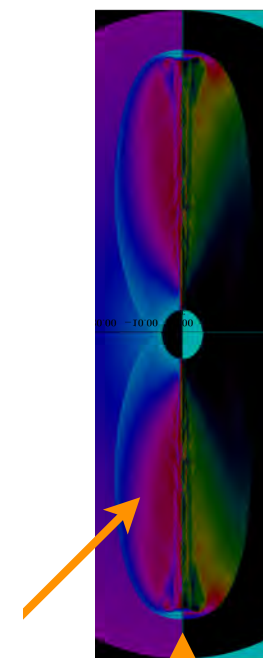


1D versus 2D



R [10¹⁰ cm]

R [10¹⁰ cm]



spectra

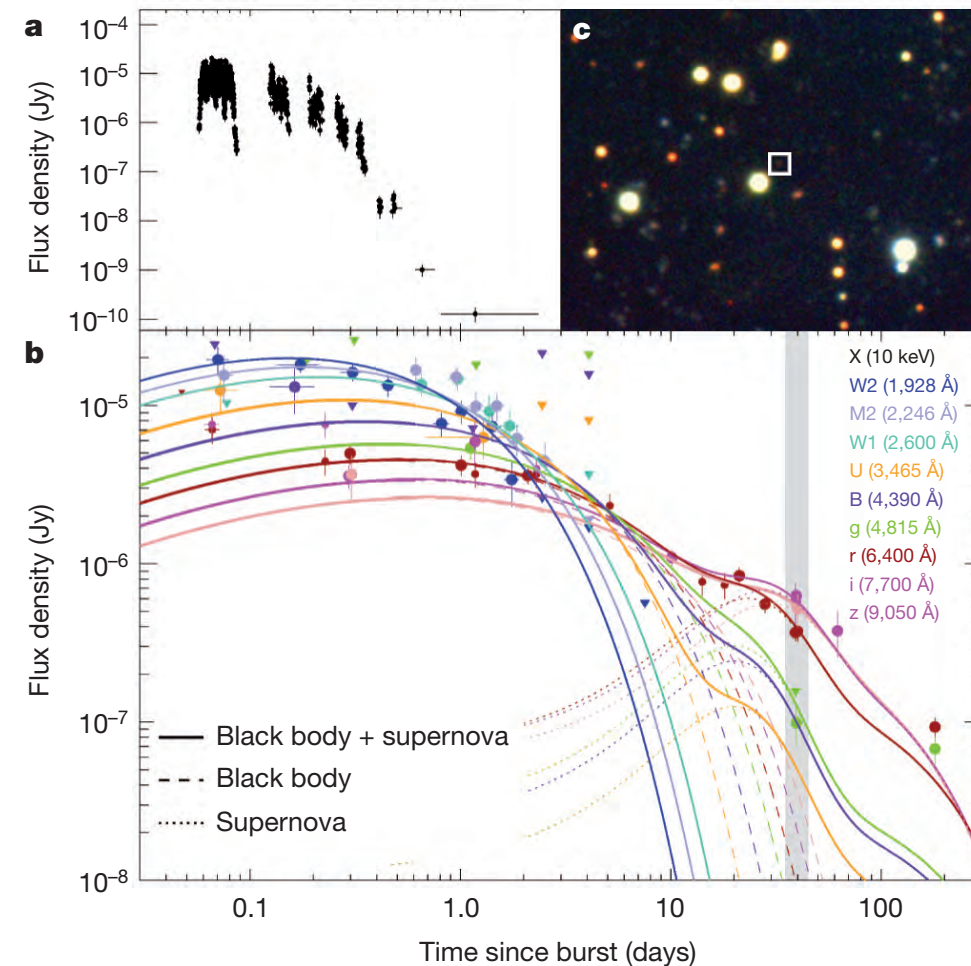
on-axis obs.

• 2D comparison
comparison with J1644+57

GRB 101225A (BB dominated GRB)

Properties:

- Its γ -ray emission was **exceptionally long-lived** ($T_{90} > 7000$ s).
- It has **no classical afterglow**: the X-ray emission following the GRB is best fitted with **blackbody + power-law** spectrum



LETTER

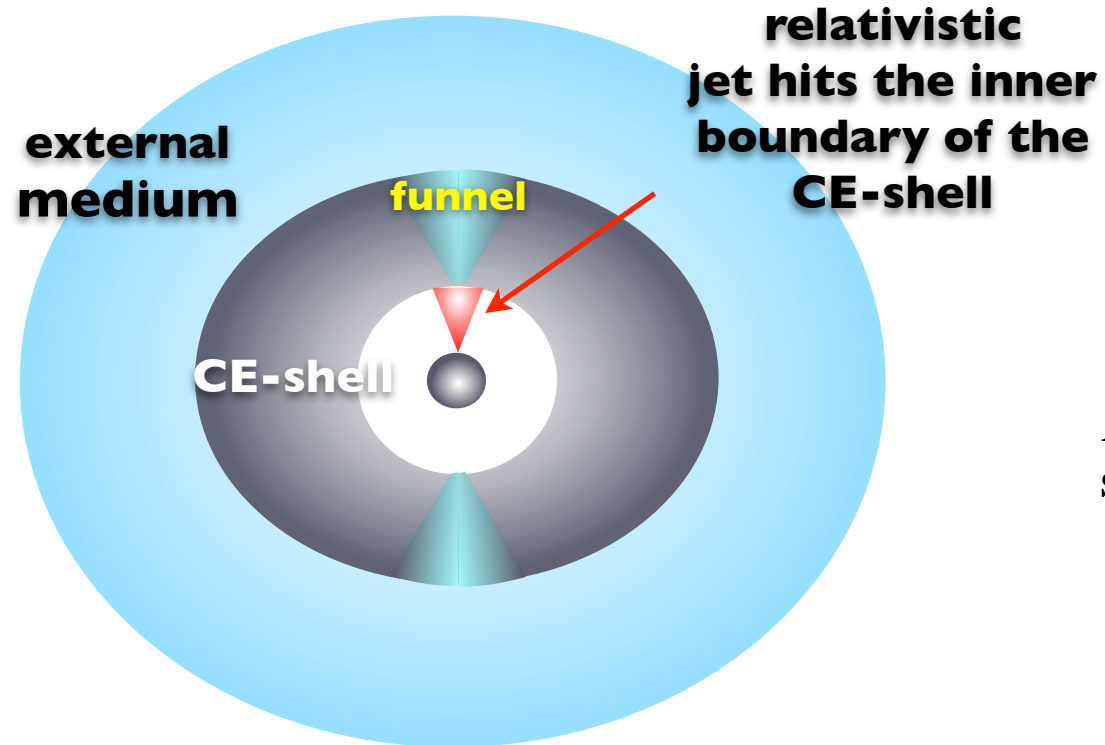
doi:10.1038/nature10611

The unusual γ -ray burst GRB 101225A from a helium star/neutron star merger at redshift 0.33

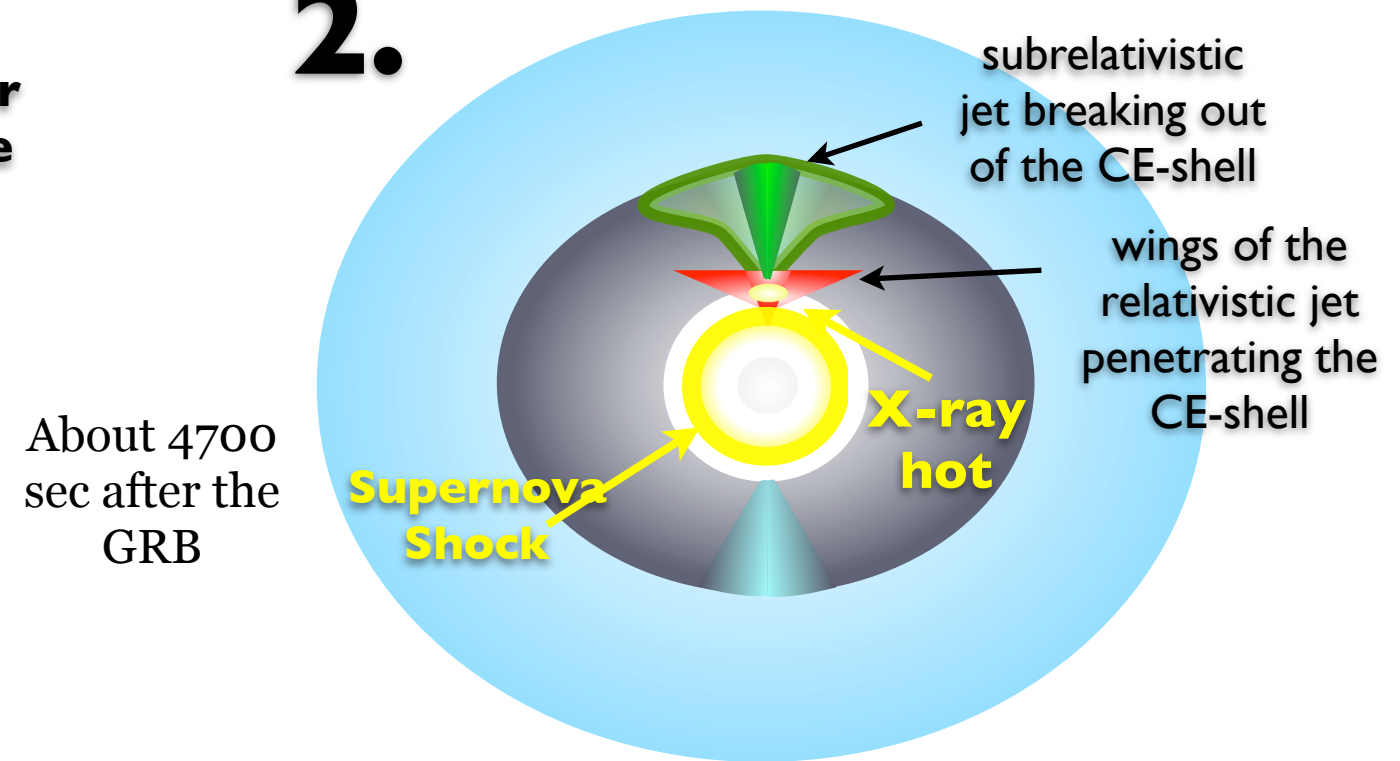
C. C. Thöne^{1,2}, A. de Ugarte Postigo³, C. L. Fryer⁴, K. L. Page⁵, J. Gorosabel¹, M. A. Aloy⁶, D. A. Perley⁷, C. Kouveliotou⁸, H. T. Janka⁹, P. Mimica⁶, J. L. Racusin¹⁰, H. Krimm^{10,11,12}, J. Cummings¹⁰, S. R. Oates¹³, S. T. Holland^{10,11,12}, M. H. Siegel¹⁴, M. De Pasquale¹³, E. Sonbas^{10,11,15}, M. Im¹⁶, W.-K. Park¹⁶, D. A. Kann¹⁷, S. Guziy^{1,18}, L. Hernández García¹, A. Llorente¹⁹, K. Bundy⁷, C. Choi¹⁶, H. Jeong²⁰, H. Korhonen^{21,22}, P. Kubánek^{1,23}, J. Lim²⁴, A. Moskvitin²⁵, T. Muñoz-Darias²⁶, S. Pak²⁰ & I. Parrish⁷

Jet-shell interaction scenario

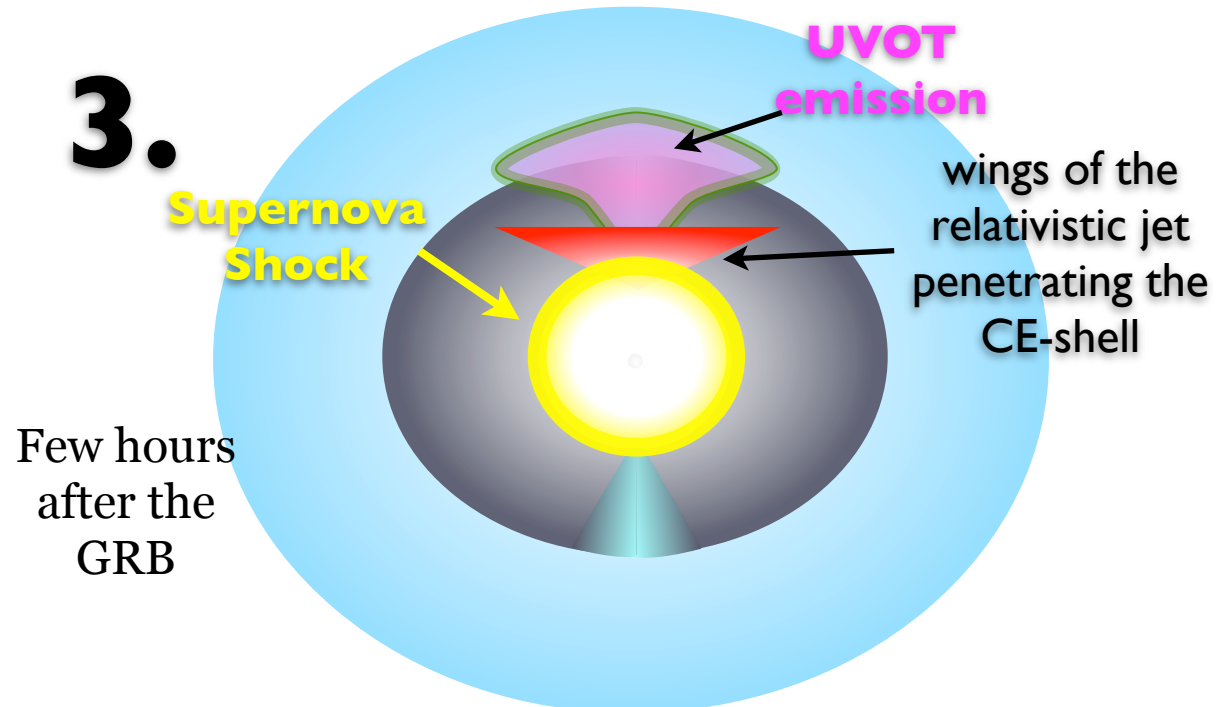
1.



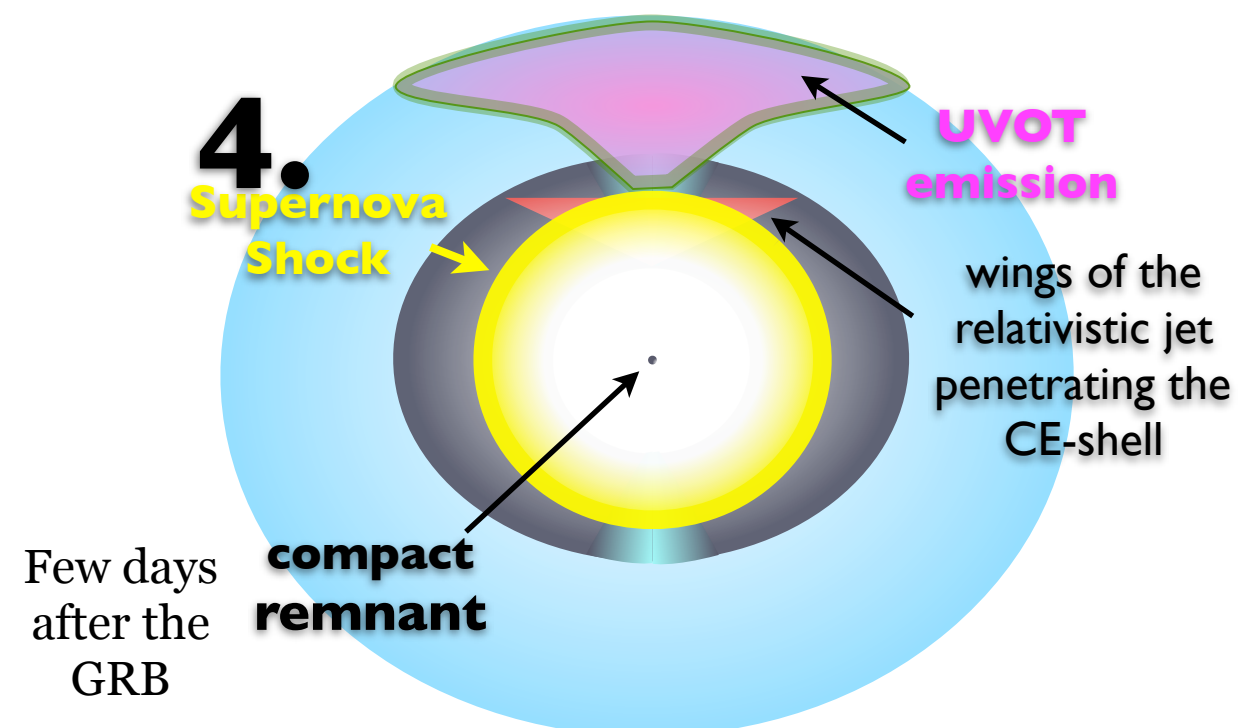
2.



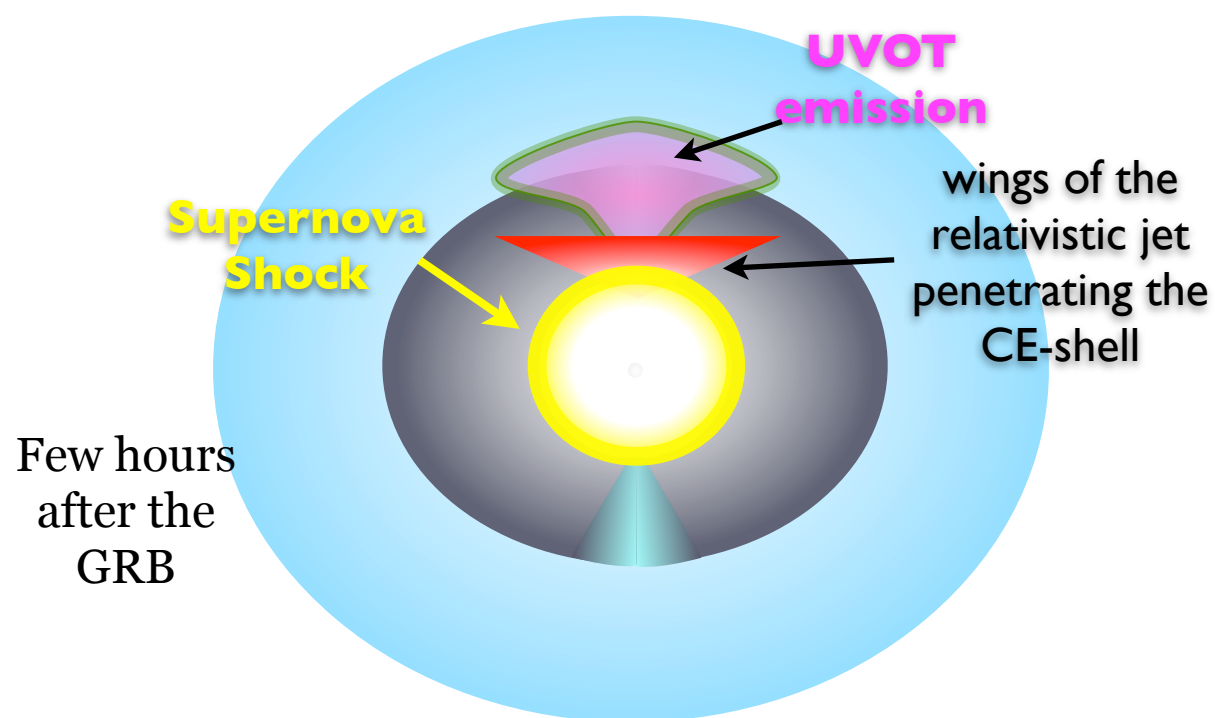
3.



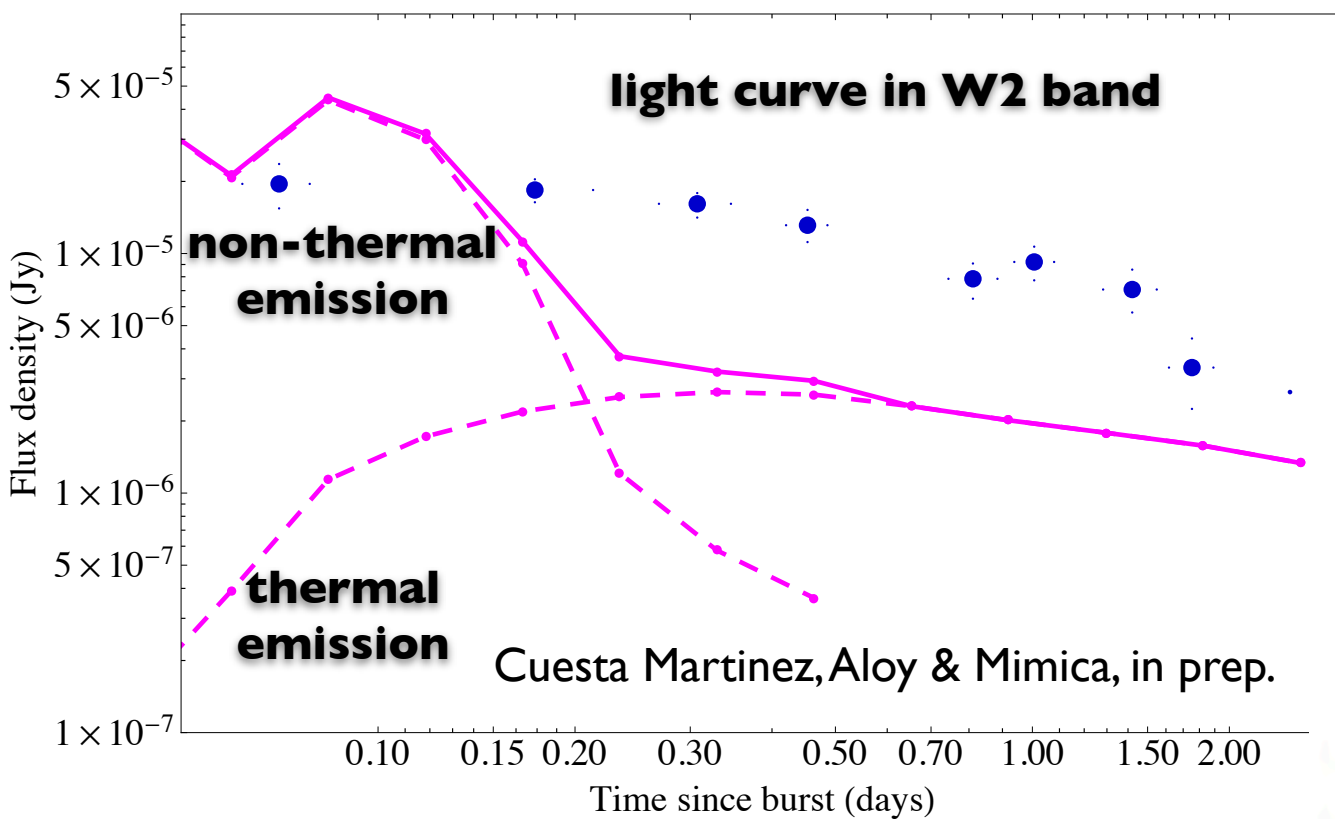
4.



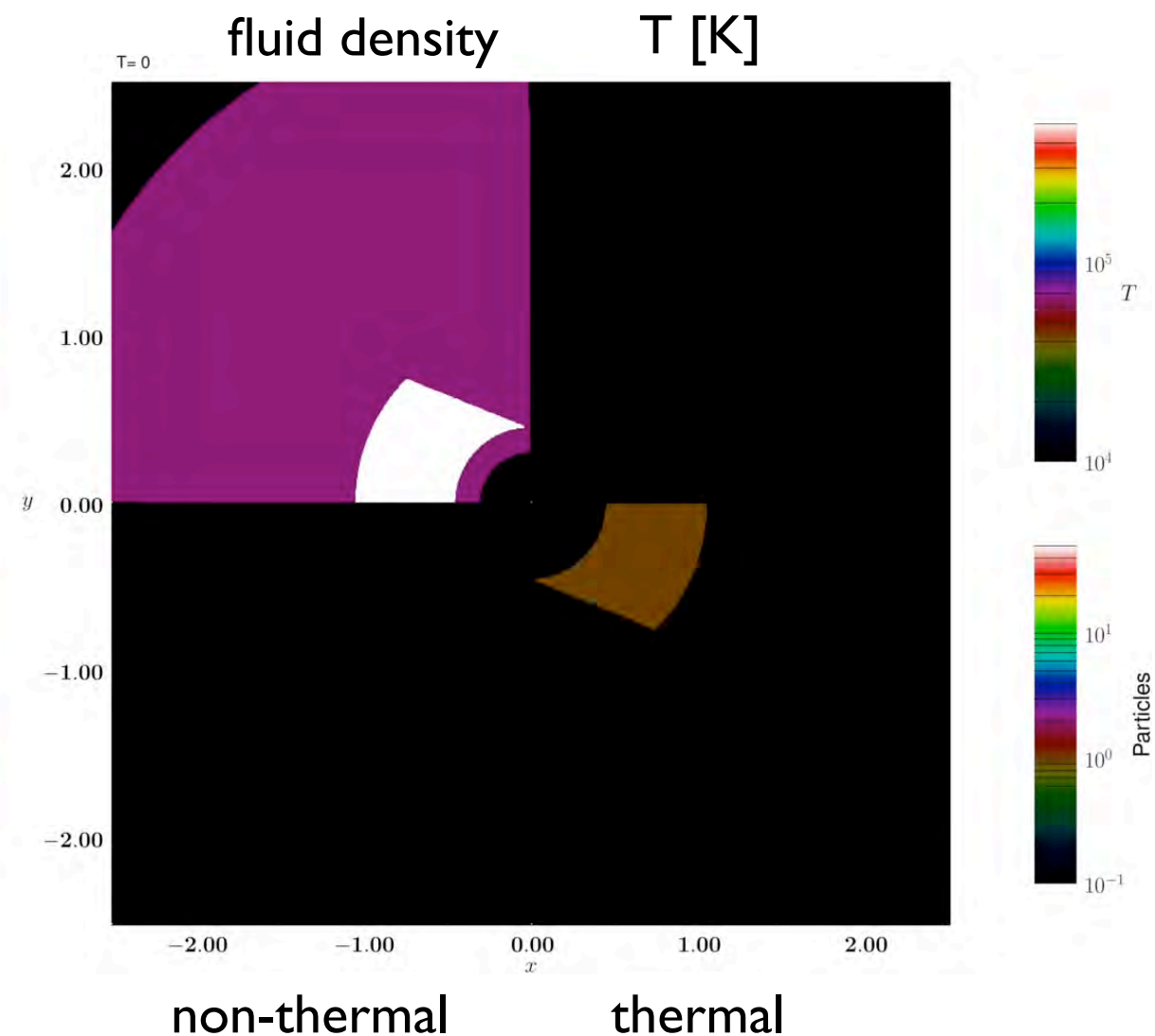
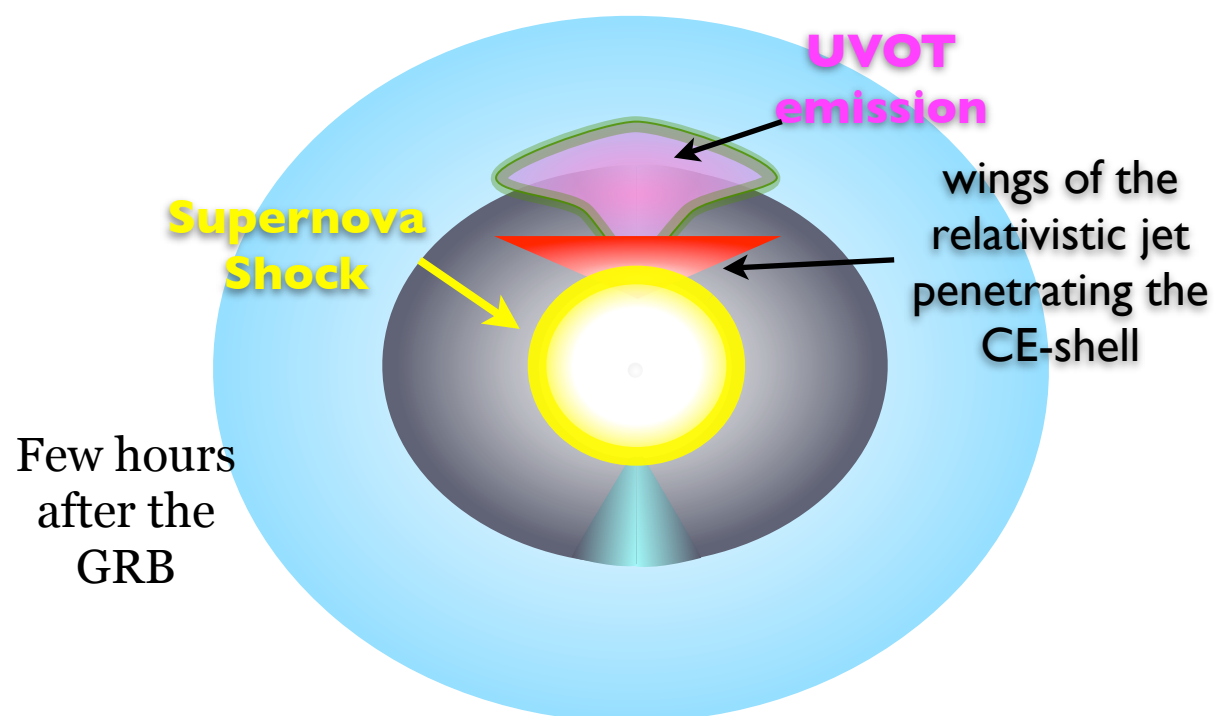
Thermal and non-thermal emission



Thermal and non-thermal emission



- thermal emission: bremsstrahlung
- opacity: modified Kramers
- non-thermal emission: synchrotron
- non-thermal absorption: SSA
- source located at $0.33 \leq z \leq 0.85$
- source observed on-axis



Summary

- **MARGENESIS+SPEV:**
 - simulation framework applied to AGN, GRB and TDE jets
 - modular and adaptable to computing at different scales
- future development:
 - technical
 - go beyond the shared-memory parallelism for particles
 - improve I/O performance
 - multidimensional shock front reconstruction
 - modeling
 - improve non-thermal particle model
 - include polarization
 - radiative transfer in GR